β-Catenin Upregulates the Constitutive and Virus-Induced Transcriptional Capacity of the Interferon Beta Promoter through T-Cell Factor Binding Sites.

Vasco Marcato, Lionel Luron, Lucie M Laqueuvre, Dominique Simon, Zeyni Mansuroglu, Marie Flamand, Jean-Jacques Panthier, Sylvie Souès, Charbel Massaad, Eliette Bonnefoy

Beta-catenin up-regulates the constitutive and virus-induced transcriptional capacity of the interferon-β promoter through T-cell factor binding sites

Vasco Marcato[1], Lionel Luron[1], Lucie M. Laqueuvre[1], Dominique Simon[3,4], Zeyni Mansuroglu[1], Marie Flamand[2], Jean-Jacques Panthier[3,4], Sylvie Souès[1], Charbel Massaad[5] & Eliette Bonnefoy[1#]

[1]Inserm UMR-S1007, Université Paris Descartes, Sorbonne Paris Cité, Paris, France; [2]Institut Pasteur, Unité de Recherche de Virologie Structurale, Paris, France; [3]Institut Pasteur, Unité de Génétique Fonctionnelle de la Souris, Paris, France; [4]Centre National de la Recherche Scientifique URA 2578, Paris, France; [5]Inserm UMR-S1124, Université Paris Descartes, Sorbonne Paris Cité, Paris, France.

Running title: TCF/β-catenin regulation of IFN-β gene expression

Word count for abstract : 192

Word count for text : 6116

Word count for Materials and Methods: 1032

[#]corresponding author: eliette.bonnefoy@parisdescartes.fr

Abstract

Rapid up regulation of interferon-β (IFN-β) expression following virus infection is essential to set up an efficient innate antiviral response. Biological roles related to the antiviral and immune response have also been associated to the constitutive production of IFN-β in naïve cells. However, mechanisms capable to modulate constitutive IFN-β expression in the absence of infection remain largely unknown. In this work we demonstrate that inhibition of kinase GSK-3 leads to the up-regulation of the constitutive level of IFN-β expression in non-infected cells, provided that GSK-3 inhibition be correlated with binding of β-catenin to the IFN-β promoter. Under these conditions, IFN-β expression occurred through the T-cell factor (TCF) binding sites present on the IFN-β promoter, independently of IRF3. Enhancement of the constitutive level of IFN-β was *per se* capable to confer an efficient antiviral state to naïve cells and acted in synergy with virus infection to stimulate virus-induced IFN-β expression. Further emphasizing the role of β-catenin in the innate antiviral response, we show here that highly pathogenic Rift Valley fever virus (RVFV) targets the Wnt/β-catenin pathway and the formation of active TCF/β-catenin complexes at the transcriptional and protein level in RVFV-infected cells and mice.

Introduction

Production of interferon-β (IFN-β) plays a central role in the induction of the innate antiviral response (1,2). Rapid up-regulation of IFN-β gene expression occurs after recognition of viral nucleic acids by pattern recognition receptors (PRRs) either cytosolic such as retinoic acid-inducible gene I (RIG-I) and melanoma differentiation-associated antigen 5 (MDA-5) or membrane-associated Toll-like receptors such as TLR3 (3). After sensing single or double stranded RNA of viral origin, these receptors activate signaling pathways implicating the phosphorylation and nuclear translocation of several transcription factors among which the interferon regulatory factor 3 (IRF3), rapidly leading downstream to a robust activation of the expression of IFN-β gene. After being secreted, IFN-β protein binds to the type I interferon receptor and triggers the JAK-STAT1/2 signal transduction pathway. This pathway leads to the activation and inhibition of the expression of a large set of genes that constitute the type I IFN response mounted to antagonize viral infection at different levels (4).

Mice lacking IFN-β (5) or the subunit of the type I interferon receptor (6,7) are highly susceptible to viral infections. They succumb to sub-lethal doses of a variety of viruses thus confirming the main role of IFN-β in the establishment of an innate antiviral response. However, beyond the antiviral response, IFN-β affects a wide range of other biological functions for the most related to modulation of the immune (innate and adaptive) and inflammatory responses as well as to cell proliferation and differentiation. Even though IFN-β has been described of anti-inflammatory benefit, it has also been implicated in the development of several inflammatory and autoimmune diseases (8-10). Hence, the beneficial or detrimental outcome of IFN-β expression for the organism will depend on the timing, the kinetics and the amount of IFN-β being synthesized (11,12). If a marked activation of IFN-β gene expression is required to efficiently set up the appropriate response to an external

aggression such as virus infection, this response needs to be adjusted in order to limit its pathological side effects.

As expected for a gene with pleiotropic functions, its transcriptional state is regulated at different levels. At the cellular level, only a stochastic fraction of the infected cells produce IFN-β (13,14) as a way to avoid an exacerbated and uncontrolled IFN response. At the nuclear level, one IFN-β allele localizes within interchromosomal regions rich in NF-κB DNA binding sites before and after infection (15) whereas the other allele localizes next to pericentromeric heterochromatin (PCH) clusters in the absence of infection and dissociates from PCH clusters during infection (16). The monoallelic characteristic of these particular subnuclear localizations suggests that a yet non-deciphered regulatory mechanism exists at the chromosome level. Finally, at the promoter level, the coordinated action of several transcription factors and chromatin remodeling complexes (17-21) regulate the IFN-β promoter transcriptional capacity. Among transcription factors, IRF3 plays an essential role during pathogen dependent activation of IFN-β gene expression in most cell types (22). Alongside with IRF3, are recruited over the promoter transcription factors such as NF-κB (15,23), ATF2/c-Jun and YY1 (20,24,25) that participate in the recruitment of chromatin remodeling complexes associated with histone acetyltransferase CBP. Some of these factors play dual roles, acting not only as activators but also as repressors of IFN-β expression. This is the case for NF-kB (26) and YY1 (27). Specially, YY1 participates in the transcriptional activation through recruitment of CBP and in the establishment of the repressive state of the IFN-β promoter through recruitment of co-repressor SAP30 (21) and association with pericentromeric heterochromatin (16).

Even though the IFN-β gene has been considered as repressed in naïve cells, low levels of IFN-β have been detected in different types of non-infected cells in the central nervous system (28,29), splenocytes and mouse embryonic fibroblasts (MEFs) (30) implying

89 the existence of mechanisms capable to regulate the production of limited amounts of IFN-β
90 in the absence of infection. Using anti-IFN-α/β antibodies, Haller et al. (31) evidenced a role
91 of such IFN-β production with respect to the establishment of an active antiviral response.
92 Using a similar strategy, Vogel and Fertsch (32) showed that the IFN-β production detected in
93 non-infected cells had an autostimulatory role upon macrophage differentiation. More
94 recently, results obtained with mice lacking either IFN-β or its receptor have confirmed the
95 physiological role of such low amounts of IFN-β produced by non-infected animals in
96 relation with several biological functions such as immune cell function, antiviral defense,
97 bone remodeling and modulation of homeostatic balance (reviewed in 33). As in the case of
98 virus-induced IFN-β production, deregulation of virus-independent IFN-β expression can lead
99 to pathological effects. However, mechanisms capable to affect IFN-β expression in the
100 absence of infection remain to be clarified.

101 In the cytoplasm, β-catenin is found within a degradation complex associated with
102 Adenomatous Polyposis Coli (APC), Axin and GSK-3 as well as CK1A Ser/Thr kinases that
103 control the level of free β-catenin by a phosphorylation-dependent targeting of β-catenin
104 towards proteasome degradation (34,35). Disruption of the degradation complex through
105 inhibition of GSK-3 kinase leads to the increase of β-catenin and its subsequent nuclear
106 accumulation. In the nucleus, β-catenin physically interacts with T-cell factor (TCF) to
107 regulate the expression of target genes through the recruitment of a transcriptional activator
108 complex containing B-Cell Lymphoma 9 (BCL9) protein and CBP over promoter regions
109 carrying binding sites for TCF factors (36-38).

110 With the goal to identify mechanisms susceptible to affect the level of IFN-β
111 expression in the absence of infection, namely IRF3-NFκB-ATF2/cJUN-independent
112 expression considered here as constitutive expression, we have questioned in this work the

capacity of nuclear β-catenin to regulate IFN-β expression, in naïve and infected cells, in association with the TCF family of transcription factors for which we show that DNA binding sites are present in the murine and human IFN-β promoter.

We demonstrate here that LiCl treatment, a potential inhibitor of GSK-3, enhanced the constitutive level of IFN-β expression provided that it would lead to the interaction of β-catenin with IFN-β promoter. While it has been previously reported that β-catenin would modulate IFN-β expression either positively (39-43) or negatively (44) through IRF3, our results uncover a new mechanism of up-regulation of the transcriptional capacity of the IFN-β promoter following LiCl treatment mediated by TCF/β-catenin complexes recruited over the IFN-β promoter region. Moreover, we show that the up-regulation of the constitutive level of IFN-β expression following LiCl treatment leads to the establishment of an efficient antiviral state protecting naïve cells against virus-induced cytopathic effect and acts in synergy with infection to increase IFN-β production. Further emphasizing the importance of TCF/β-catenin complex formation in the antiviral response, we show here that the pathogenicity induced by Rift Valley fever virus (RVFV) infection of cell cultures and mice was correlated with viral targeting of the TCF/β-catenin pathway at different levels.

Materials and Methods

Virus, Cells and Mice

Stocks of RVFV ZH548 and RVFV ZHΔNSs were produced under BSL3 conditions by infecting Vero cells at m.o.i. of 10^{-3} and by harvesting the medium at 72 hr p.i. Murine fibroblastic L929 cell line and NDV infections were described previously (45). Murine hepatocyte AML12 cell line was from ATCC (ref. CRL-2254). For preparation of bone marrow-derived macrophages (BMDM) preparation, bone marrow from tibiae and femora of 8-12 weeks B6 mices was flushed and cultured for 7 days in DMEM containing 10% heat-inactivated fetal bovine serum, 100 U/ml penicillin/streptomycin, 2 mM glutamine and 10 ng/ml murine M-CSF (Peprotech). Infection of mice was performed as previously described (46). When indicated, LiCl, iCRT3 (Sigma) or LiCl+iCRT3 were directly added to the culture medium.

Antibodies

Mouse anti-NSs and rabbit anti-N polyclonal antibodies were raised respectively against the entire NSs or N protein (47). Anti-β-catenin from BD Transduction laboratories (Cat#610154) was used for immunofluorescence, Western blot and gel retardation. Secondary antibodies used for immunofluorescence were Alexa 488 fluor-conjugated chicken anti-mouse from Invitrogen (A21200) and Alexa 555 fluor-conjugated donkey anti-rabbit from Invitrogen (A31572). Secondary antibodies used for Western blot were ECL Mouse IgG, HRP-linked whole Ab (NA931) an ECL Rabbit IgG, HRP-linked whole Ab (NA934) from GE Healthecare Life Sciences.

Immunofluorescence

For immunofluorescence, cells grown in 6-well plates on coverslips were fixed with 4% formaldehyde in PBS for 15 minutes and permeabilized with 1% Triton X-100 in PBS for 20 minutes. Then cells were incubated for 1 hour at room temperature with the corresponding primary antibodies diluted in PBS/BSA 5%. Cells were then washed with PBS and incubated for 1 hour at room temperature with corresponding secondary antibodies.

Image acquisition and manipulation

Samples were analyzed at room temperature by confocal laser scanning microscopy using a Zeiss LSM710 confocal system at the *Service Commun de Microscopie* (SCM) of Université Paris Descartes. This system is equipped with a 63x, 1.4 O.N oil immersion lens (Plan Neofluor). For oil immersion microscopy, we used oil with refractive index of 1.518 (Zeiss). Image capture was carried out with a definition of 1024x1024 pixels with 8 bit data for each color. Images were analyzed using Image J software. Total pixel intensity was quantified using Image J software.

Chromatin immunoprecipitation

Chromatin immunoprecipitation experiments were carried out as previously described (21). PCR analysis of inputs or immunoprecipitated DNAs was performed using oligonucleotides F-40 (5'-GTT TTC CCA GTC ACG AC-3') and CAT (5'-CCA TTT TAG CTT CCT TAG-3') to reveal the integrated WT330 and WT110 IFN-β promoter. For the F-40, CAT set of primers, PCR conditions were as follows: 1 cycle of 94°C for 5 minutes; 20 cycles of 94°C for 30 seconds, 53°C for 30 seconds and 72°C for 30 seconds; 1 cycle of 72 °C for 10 minutes. A first "cold" PCR was carried out in the presence of 25 pmol of each primer; 1.5 µl

of the product of the first PCR was subjected to a second "hot" PCR carried out in the presence of 0.1 µl a-^{32}PdATP (6000 Ci/mmol) and 25 pmol of each primer.

RT-qPCR

Total RNA was extracted using Tri Reagent (Sigma) according to the manufacturer's protocol. 1 µg of total RNA was reversely transcribed using High Capacity cDNA Reverse Transcription Kit (Applied Biosystems) according to the manufacturers' recommendations using Random Primers. qPCR was performed using SYBR Green (Thermo Scientific) reagents: 95°C 15 minutes, then 40 cycles at 95°C 15 seconds, 60°C 1 minute, followed by a dissociation step. Relative quantification of mRNA expression was calculated using the $\Delta\Delta C_T$ method using three reference genes among Ppib, Hprt1, Utp6c and Rplp0). For fold changes lower than 1 (translating a repression of the gene's expression), the inverted values were determined such that a 0.5 fold change corresponds to -2. Sequences of primers used for RT-qPCR analysis are shown in Table I.

Statistical analysis was carried out using Student T-test or the REST software that uses a Pair-Wise Fixed Reallocation Randomization Test© to determine a P-value.

RNA interference experiments

L929 cells were transfected using Lipofectamine 2000 (Invitrogen Life Technologies) with the ON Target Plus SMART Pool of siRNA oligos specific for β-catenin (Thermo Scientific Dharmacon® L-040628-00) or with a pool of control siRNA sequences (Thermo Scientific Dharmacon® D-001810-10-05) at a final concentration of 50nM each during 72 h.

Gel retardation assay

Nuclear extracts of murine L929 cells either non-treated or treated with LiCl for 24 h were incubated with the corresponding 5' ^{32}P-labeled probes in 20 µl (final volume) of 50 mM Tris-HCl (pH 7.5), 50 mM NaCl, 5 mM EDTA, 10% glycerol and 5 mM dithiothreitol. When indicated, anti-β-catenin antibody was incubated with the nuclear extracts 1 h at 4°C prior to the addition of the labeled probe.

Cytopathic effect assays.

Monolayer cultures of L929 cells in 96-well plates were incubated with LiCl for 24 h before VSV infection. Before VSV infection, the medium containing LiCl was removed. Viruses were diluted in medium with serum (2% final concentration) and added directly to the culture medium. The monolayers were stained with crystal violet as vital dye 24 h after VSV infection or fixed 8h after VSV infection for immunofluorescence analysis. For measurement of the cytopathic effet of RVFV, L929 cells either non-treated or treated with LiCl for 24 h were infected with RVFVZH548 and incubated under an overlay consisting of DMEM, 2% fetal calf serum, antibiotics and 1% agarose at 37°C. At 3 day p.i., the lytic plaques were counted after staining with a solution of crystal violet.

Western blot

For Western blot, total protein extracts were prepared in RIPA buffer and resolved by sodium dodecyl sulfate-polyacrylamide gel electrophoresis (SDS-PAGE) in 4-12% precast gels (Life Technologie). Relative quantification of proteins was carried out using Image Quant software on scanned WB films.

Ethics Statement

227 Experiments on live mice were conducted according to the French and European
228 regulations on care and protection of laboratory animals (EC Directive 86/609, French Law
229 2001-486 issued on June 6, 2001) and the National Institutes of Health Animal Welfare
230 (Insurance #A5476-01 issued on 02/07/2007). Experimental protocols were approved by the
231 Animal Ethics Committee #1 of the *Comité Régional d'Ethique pour l'Expérimentation*
232 *Animale* (CREEA), Ile de France (N°2012-0025), and carried out in compliance with Institut
233 Pasteur Biosafety Committee.
234

Results

LiCl treatment enhances constitutive IFN-β gene expression.

The proximal region of the IFN-β promoter (Fig. 1A), made of negative and positive regulatory domains, is highly conserved between murine and human cells. The Virus Responsive Element (VRE) that contains binding sites for transcription factors IRF3, ATF2/c-Jun, NF-κB and YY1 is surrounded by two Negative Regulatory Domains (NRDI and II) described as regions of nucleosome positioning (18). Sequence analysis of the murine IFN-β promoter revealed the presence in the NDRII of two potential DNA-binding sequences for TCF transcription factors. A first site, TCFa, between positions -374 and -367 (5'-TTCAAAGG-3') that perfectly matches the consensus TCF DNA binding sequence 5'-(A/T)(A/T)CAAAGG-3' (38). A second site, TCFb, between positions -233 and -226 (5'-CCTTTGcT-3') that differs from the consensus TCF DNA binding sequence by one base. Two sequences homologous to the murine TCFb sequence are present in the human IFN-β promoter, between positions -260 and -253 and +26 and +33 respectively.

The presence of potential TCF binding sites within the proximal region of the IFN-β promoter suggested that expression of the IFN-β gene could be modulated in response to pathways inducing nuclear accumulation of β-catenin and formation of TCF/β-catenin complexes over the IFN-β promoter region. In order to test this hypothesis, we analyzed IFN-β gene expression in non-infected cells, corresponding to an IRF3-NF-κB-ATF2/c-Jun independent expression that we have considered as constitutive IFN-β expression, before and after nuclear accumulation of β-catenin. Experiments were carried out in murine fibroblastic L929 cells, which are potent IFN-β producer cells. In the absence of GSK-3 inhibition, little if any β-catenin was detected in the nucleus of L929 cells whereas the nuclear distribution of β-catenin was significantly enhanced after treatment of the cells with LiCl, an inhibitor of GSK-

3 (Fig. 1B-D). IFN-β gene expression measured by RT-qPCR in LiCl-treated cells compared to untreated cells, showed that LiCl treatment significantly enhanced the constitutive level of IFN-β mRNAs ($p<10^{-5}$) (Fig. 1E) independently of any virus infection. Even though the level of IFN-β expression measured after LiCl treatment was much lower than that induced during viral infection (16), it was sufficient to trigger an IFN-β response as reflected by a significant induction of the expression of two major IFN-stimulated genes (ISGs), *Oas1b* and *Irf7* genes (Fig. 1F). The effect of LiCl on IFN-β expression was dose dependent. The highest effect, before reaching saturation, was observed at 20 mM LiCl (Fig. 1G).

Low constitutive levels of IFN-β have been previously shown to synergize with virus infection for efficient virus-induced IFN-β production (30,48). In order to test if the enhancement of the constitutive level of IFN-β gene expression induced by LiCl in naïve cells could affect virus induced IFN-β expression, L929 cells were either pretreated or not with LiCl before being infected with Newcastle Disease Virus (NDV) that, contrary to LiCl, does not induce the nuclear accumulation of β-catenin (Fig. 1H and J). As shown in Fig. 1J, pretreatment of the cells with LiCl significantly potentiated NDV-induced IFN-β expression.

The effect of LiCl treatment on IFN-β expression is mediated by β-catenin.

In order to confirm that the effect of LiCl treatment on constitutive IFN-β expression was not due to LiCl treatment *per se* but required the nuclear accumulation of β-catenin, we made use of murine hepatocyte AML12 cells that produce IFN-β in response to viral infection but, by contrast to L929 cells, do not accumulate nuclear β-catenin after LiCl treatment (Fig. 2A and B). Measurement of the expression of IFN-β mRNA in AML12 cells either treated or not with LiCl, before (Fig. 2C) and after (Fig. 2D) NDV infection, showed that the inability of LiCl to induce the accumulation of nuclear β-catenin in this particular cell type correlated

283 with the inability of LiCl treatment to enhance IFN-β expression either in the absence
284 (Fig.2C) or presence (Fig. 2D) of virus infection.

285 The role of β-catenin during LiCl enhancement of IFN-β expression was further
286 confirmed using siRNAs. For this, L929 cells were mock-transfected or transfected either
287 with siRNAs directed against β-catenin or with control siRNAs (Fig. 2E-G) before being
288 treated with LiCl for 24h. Under conditions of diminution of β-catenin mRNA (Fig. 2E) and
289 protein (Fig. 2F) level, we observed that LiCl treatment had no significant effect on IFN-β
290 expression compared to cells treated with control siRNAs (Fig. 2G) confirming therefore that
291 the capacity of LiCl treatment to activate IFN-β expression was mediated by β-catenin.
292

293 **LiCl treatment stimulates the recruitment of β-catenin on the IFN-β promoter through**
294 **the NRDII promoter region containing a TCF binding site.**

295 IRF3 transcription factor is known to promote IFN-β expression, yet its activation,
296 nuclear translocation and subsequent IFN-β promoter binding, require the previous activation
297 of PRRs. The capacity of LiCl treatment to affect IFN-β gene expression in the absence of
298 infection showed that activation of the transcriptional capacity of the IFN-β promoter could
299 occur independently of IRF3, through a mechanism that we hypothesized to be TCF/β-
300 catenin-dependent. In order to test this hypothesis, we made use of previously established
301 L929 cell lines carrying integrated into their genome the proximal IFN-β promoter region
302 fused to the CAT reporter gene either from positions -330 to +20 (L929 WT330 cells) or from
303 positions -110 to +20 (L929 WT110 cells) (45). The NRDI region and the entire VRE region,
304 containing the IRF3 binding site, are present in both promoters whereas the NRDII region,
305 containing a TCF binding site, is only present on the WT330 promoter (Fig. 3A). Therefore,
306 contrary to the WT330 promoter that contains a TCF binding site, no TCF binding site is
307 present in promoter WT110.

ChIP analysis presented in Fig. 3B indicates that LiCl treatment induced β-catenin binding to the WT330 promoter but not to the WT110 promoter, demonstrating that β-catenin binding to the IFN-β promoter that occurred in the absence of virus infection required the NRDII region containing a TCF binding site.

If, as hypothesized, the activation of IFN-β expression induced after LiCl treatment required the recruitment of β-catenin on the IFN-β promoter, then only the WT330 promoter was expected to respond to LiCl treatment. In order to test this prediction, we pretreated L929 WT330 and WT110 cells with LiCl and assayed the corresponding CAT activities (Fig. 3C). As expected, LiCl treatment enhanced by 4-folds the constitutive transcriptional capacity of the WT330 promoter, but not that of the WT110 promoter. Thus reinforcing the indispensable role of the promoter region positioned 5' of the VRE, containing a TCF binding site, for LiCl treatment to enhance the constitutive transcriptional capacity of the IFN-β promoter.

The role of the NRDII region containing a TCF binding site during LiCl-dependent promoter activation was also analyzed after virus infection. As shown in Fig. 3D, LiCl treatment enhanced the virus-induced activity of the WT330 promoter, but not that of the WT110 promoter. Therefore, the presence of the NRDII region containing a TCF-binding site was also required for the LiCl-dependent enhancement of the virus-induced transcriptional capacity of the IFN-β promoter. The presence of only the VRE region, containing the IRF3 binding site (promoter WT110), was not sufficient to either recruit β-catenin or mediate LiCl enhancement of the constitutive as well as virus-induced transcriptional capacity of the IFN-β promoter.

LiCl that is considered as an inhibitor of GSK-3 can also affect the activity of other kinases. In order to further investigate if the effect of LiCl on IFN-β expression was the consequence of the inhibition of GSK-3, L929wt330 and wt110 cells were treated with two other inhibitors of GSK-3, SB216763 and inhibitor IX. Similarly to LiCl, a dose dependent

activation of the transcriptional capacity of the WT330 promoter was observed in the presence of increasing amounts of SB216763 (Fig. 3E). Also, treatment with either SB216763 or inhibitor IX had the same effect than LiCl, activating the transcriptional capacity of WT330 promoter but not that of WT110 promoter (Fig. 2E and F). Since GSK-3 is a common target for these three inhibitors, the fact that LiCl, SB216763, and inhibitor IX had the same effect on the transcriptional capacity of the IFN-β promoter strongly supports the hypothesis that LiCl dependent enhancement of IFN-β expression is the consequence of the inhibition of GSK-3.

The effect of LiCl treatment on IFN-β expression is mediated by TCF.

Gel retardation assays were used to analyze the capacity of TCF binding sites present within the NRDII region of IFN-β promoter to form complexes displaying the characteristics of TCF-DNA complexes. For this, we used oligonucleotides containing the sequence of wild-type, mutated TCFa or mutated TCF b sites. TCF binding sites were mutated in their core motif containing the stretches of A required for the HMG box of TCF factors to interact with DNA. The TCFa site was mutated to give rise to TCFmutA (5'-TTC*gg*AGG-3') site and the TCFb site was mutated to give rise to TCFmutB (5'-CC*cc*TGcT-3') site. The corresponding radioactively labeled, double-stranded DNA probes were incubated with nuclear extracts prepared from L929 cells either non-treated or treated by LiCl during 24h. Whereas complex formation was only weakly observed in the presence of nuclear extracts from non-treated cells, a protein-DNA complex (indicated by an arrow in Fig. 4A) was clearly formed when the DNA probes containing the wild-type TCFa or TCFb sites were incubated with nuclear extracts from LiCl treated cells. As expected for a TCF-DNA complex, complex formation was disrupted when the core region of the TCF DNA binding sequence was mutated as in TCFmutA and mutB probes (Fig. 4B). T-Cell Factors interact with the minor groove of A/T

base pairs through their HMG-box and therefore are known to display affinity for I/C sequences that resemble A/T sequences in the minor groove (49, 50). Therefore, as expected for a TCF-DNA complex, the previous incubation of nuclear extracts with non-labeled polydI/dC sequences inhibited complex formation with the radioactively labeled TCFA probe (Fig. 4B). Finally, incubation of the nuclear extracts with anti-β-catenin antibodies affected the formation of the protein-DNA complex that in the presence of antibodies was less intense and supershifted (Fig. 4B), indicative of the presence of β-catenin within the complex.

To confirm the role of TCF binding sites in the LiCl dependent activation of the IFN-β promoter transcriptional capacity, the IFN-β promoter region from positions -458 to +36 either wild-type or mutated in one or both TCF binding sites was cloned in front of the luciferase reporter gene. After transfecting the corresponding plasmids into L929 cells, the transfected cells were either treated or not with LiCl before being infected with NDV. The corresponding luciferase activities were measured (Fig. 4C). Contrary to wild-type and mutB promoters whose corresponding transcriptional capacities could be activated following LiCl treatment, promoter mutA partially lost its capacity to be activated by LiCl and no activation was observed in the case of the promoter mutAB. Therefore, results obtained here with TCF mutated promoters demonstrated that the presence of at least one TCF binding site was required for LiCl to activate the transcriptional capacity of the IFN-β promoter. In the context of the promoter region cloned in these constructions (from -458 to +36), the TCFa that perfectly matches the consensus sequence site appeared more efficient than the TCFb site.

In order to definitively confirm the role of TCF/β-catenin complexes during LiCl enhancement of the transcriptional capacity of the endogenous IFN-β promoter, we used iCRT3, which is a potent inhibitor of TCF4/β-catenin complexes (51). The presence of IFN-β mRNAs was measured in NDV-infected L929 cells that were either non-treated or pretreated with LiCl during 24 or 48 h in the absence or presence of different amounts of iCRT3

corresponding to the range of iCRT3 concentration necessary to inhibit TCF/β-catenin dependent transcription of the Axin-2 and CycD1 (51). A dose-dependent inhibition of the effect of LiCl on IFN-β expression was observed in the presence of iCRT3, and this in the case of 24h as well as 48h (Fig. 4D) of LiCl treatment. In the same samples, iCRT3 also inhibited the activation of the expression of the gene coding for CyclinD1 (Fig. 4E), which is known to be regulated by TCF/β-catenin complexes. Overall demonstrating that the capacity of LiCl to enhance IFN-β expression was mediated by TCF/β-catenin complexes.

LiCl treatment confers an efficient antiviral response.

Fig. 1E shows that LiCl-dependent enhancement of the constitutive level of IFN-β expression was sufficient to lead to a significant activation of the expression of two major ISGs, *Oas1b* and *Irf7*, responsible for the RNaseL-dependent degradation of viral ARN and for the amplification of the IFN-β response respectively. In order to analyze the efficiency of such LiCl-induced interferon response with respect to the establishment of an antiviral state, we compared the cytopathic effect (CPE) of Vesicular Stomatitis Virus (VSV) in murine L929 cells either pretreated or not with LiCl. Indeed, following infection of murine L929 cells with VSV, cell viability is expected to decrease as the amount of VSV increases unless an efficient IFN-β response had been mounted previously to VSV infection (52).

L929 cells pretreated or not with LiCl were infected with increasing titers of VSV. Twenty-four hours after infection, the cells were stained with crystal violet, which detects CPE as a decrease in staining intensity. As shown in Fig. 5A, at low multiplicity of infection (MOI), cells pretreated with LiCl displayed less VSV-induced CPE than untreated cells, highlighting the capacity of LiCl treatment to induce an efficient antiviral response protecting cells against VSV-induced cell death. The capacity of LiCl treatment to confer an efficient antiviral response at low MOI is further depicted in photographs of culture fields of LiCl-

408 treated versus untreated cells 24h after post infection (p.i.). Whereas the majority of non-
409 treated cells died 24h p.i., LiCl-treated cells grew to confluence displaying resistance to
410 infection (Fig. 5B).

411 Even though at higher MOI all cells died by 24 h p.i. regardless of LiCl treatment (Fig.
412 5A), at a MOI of 1 the percentage of cells detected as infected by fluorescent staining was
413 significantly lower at earlier times after infection (8h p.i.) among LiCl-treated cells than
414 among untreated cells (Fig. 5C and D). This is indicative of the capacity of LiCl-treated cells
415 to dampen the kinetics of virus multiplication.

416

417 **The canonical Wnt/β-catenin pathway is a major target of Rift Valley fever virus.**

418 Cellular pathways participating in the establishment of an effective antiviral response
419 are expected to be affected during viral infections: either "positively", leading to the
420 activation of the host antiviral response, or "negatively", in the case of viruses capable to
421 efficiently inhibit the cellular antiviral response. Therefore, if as suggested in this work, a
422 TCF/β-catenin transcription complex participates in the establishment of an efficient antiviral
423 response then pathways regulating active TCF/β-catenin complex formation are expected to
424 be targeted during viral infection.

425 The effect of a viral infection upon the canonical Wnt/β-catenin pathway, which is a
426 major regulator of the formation of active TCF/β-catenin complexes, was analyzed here
427 during infection with Rift Valley fever virus (RVFV) for which two different strains,
428 pathogenic and non-pathogenic are available. The wild type RVFV ZH548 strain (ZH) of the
429 virus that codes for a non-structural NSs protein, suppresses IFN-β expression and is highly
430 pathogenic causing severe illness in humans and animals (53-55), whereas the RVFV
431 ZH548ΔNSs strain (ΔNSs), deleted for the region coding for NSs protein, strongly activates
432 IFN-β expression and is fully avirulent (56).

433 The viral NSs protein, which is a major factor responsible of RVFV pathogenicity, has
434 the characteristic to form filamentous structures in nuclei of infected cells abnormally
435 trapping within these structures transcription factors and co-factors of the host (21,57).
436 During a recent genome wide search for regulatory DNA regions of the host interacting with
437 RVFV NSs protein, several genes associated with the canonical Wnt/β-catenin pathway were
438 identified as interacting with NSs (Table II) (58). Among these were genes coding for several
439 WNT ligands (*Wnt1*, *Wnt2*, *Wnt6* and *Wnt8b*), for antagonists of Wnt signaling (*Apcdd1*,
440 *Dkk1* and *Kremen2*), for members of the multiprotein complex regulating the degradation of
441 β-catenin (*Gsk3b*, *Gsk3a* and *Axin2*), for β-catenin itself (*Ctnnb1*) as well as for members of
442 the TCF/β-catenin complex (*Tcf7l2*, *Lef1* and *Bcl9*). Also, DNA regulatory sequences
443 associated with genes coding for casein kinases (*Csnk1d*, *Csnk1g2*, *Csnk1g3* and *Csnk2a2*)
444 known to positively regulate the canonical Wnt/β-catenin signaling pathway at different
445 levels were present among cellular DNA regions targeted by NSs.
446 Using RT-qPCR, we analyzed the effect of RVFV infection, either pathogenic (ZH
447 strain) or non-pathogenic (ΔNSs strain), upon the expression of the genes related to canonical
448 Wnt/β-catenin pathway identified as significantly interacting with NSs. For this, RNA was
449 purified from three different cell types targeted by RVFV (L929 fibroblasts, AML12
450 hepatocytes and bone marrow derived macrophages (BMDM)) either non-, ΔNSs- or ZH-
451 infected. After reverse transcription, the fold change in the expression level of genes of
452 interest (including the gene coding for IFN-β) was calculated with respect to non-infected
453 cells using three different reference genes (Fig. 6).
454 As expected, infection with the avirulent ΔNSs strain strongly activated IFN-β gene
455 expression in the three cell types tested, whereas infection with the virulent ZH strain
456 maintained the IFN-β expression in an abnormally repressed state.

457 Both strains affected the Wnt/β-catenin pathway but with opposite effects. Infection
458 with the non-pathogenic ΔNSs strain led to i) the activation of the expression of genes coding
459 for casein kinases, with *Csnk1d* and *Csnk2a2* genes activated in the three cell types tested,
460 and *Csnk1g3* activated in fibroblasts and BMDM; ii) the activation of the expression of genes
461 coding for factors essentials for the formation of an active β-catenin transcription complex
462 such as *Bcl9* and *Tcf7l2* in hepatocytes and BMDM; and iii) the repression of the expression
463 of the *Axin2* gene, a negative regulator of the canonical Wnt/β-catenin pathway (59), in
464 hepatocytes. On the contrary, infection with ZH led in BMDM to the inhibition of the
465 expression of *Csnk1d* and *Csnk2a2* genes, and the activation of the expression of *Axin2* gene.
466 Also, a slight inhibition of the expression of *Bcl9* gene was observed in fibroblasts and
467 hepatocytes.
468 As shown in Fig. 7, all the effects observed after non-pathogenic ΔNSs infection
469 tended towards the formation of an active nuclear β-catenin complex. On the contrary, the
470 effects observed after infection with the pathogenic ZH strain of the virus tended against the
471 formation of a nuclear β-catenin transcription complex.
472 Virus-induced IFN-β expression depends on the presence of several transcription
473 factors and co-factors that synergize to give rise to a maximum of expression (16-27).
474 Therefore, even though TCF/β-catenin complexes could participate on the induction of IFN-β
475 expression, they should not be considered as alone responsible of the strong IFNβ expression
476 induced during infection by ΔNSs. Similarly, even though RVFV targeting of TCF/β-catenin
477 complex formation could be participating in the RVFV-induced inhibition of IFN-β
478 expression, this should not be considered as alone responsible of the complete lack of IFN-β
479 expression in RVFV infected cells that we have previously shown to be related to the capacity
480 of NSs to maintain the IFN-β promoter region associated to a transcriptionally repressive
481 environment (16, 21).

Nevertheless, the fact that avirulent and virulent strains of RVFV had opposite, mirror, effects upon the Wnt/β-catenin pathway suggested that this pathway could be playing a role in mounting an efficient innate antiviral response against RVFV infection.

A potential role for β-catenin protein in setting up an antiviral response against RVFV infection.

In order to test the effect of RVFV infection upon the level of β-catenin *in vivo*, the presence of β-catenin was analyzed in the liver and brain of mice that were either non-infected, or infected with ΔNSs or ZH strains. Of note, the liver and brain are two main organs targeted during RVFV infection (60). Mice were euthanized at days 3 and 5 p.i. and the liver and brain were removed; one half of each organ was used for total protein purification and Western blot analysis and the other half for RNA purification and RT-qPCR analysis. Whereas no variation was observed for β-catenin at the transcriptional level (data not shown), Western blot analysis showed significant variations at the protein level in the liver of ZH-infected mice at day 5 p.i. (Fig. 8A). Under these conditions, the average relative level of β-catenin significantly diminished in the liver of all ZH-infected mice compared to non-infected and ΔNSs-infected mice where on the contrary, the level of β-catenin was increased in ΔNSs-infected mice (Fig. 8A).

Viral targeting of β-catenin was further analyzed with respect to the presence of the virus (as translated by the presence of viral mRNAs coding for viral proteins N and NSs) in the liver and the brain of each mouse under each condition. In the case of ZH-infected mice, viral N and NSs mRNAs were clearly detected at day 5 p.i. in the liver of mouse #1, 2 and 3 and by day 3 p.i. in the liver of mouse #1 (Fig. 8B) but remained essentially undetectable in the brain of infected mice. Therefore, the effect of RVFV infection upon the level of β-

506 catenin appeared correlated with the presence of the virus suggesting that β-catenin could be
507 playing a role protecting against ZH replication.

508 If as hypothesized β-catenin played a role in the antiviral response against RVFV
509 infection, then LiCl treatment should have a protective effect. In order to test this, L929 cells
510 were either non-treated or pretreated with LiCl during 24 h before infection with the virulent
511 ZH strain of RVFV. In agreement with a potential physiological role for β-catenin inhibiting
512 RVFV replication, pretreatment with LiCl significantly diminished the number of lytic
513 plaques induced by RVFV (Fig. 8C).

514

Discussion

In this work we have demonstrated that cell treatment with LiCl, an inhibitor of GSK-3, leads to the enhancement of the constitutive (namely IRF3-NFκB-ATF2/cJUN-independent) as well as virus-induced level of IFN-β gene expression, provided that LiCl treatment be correlated with the IFN-β promoter recruitment of β-catenin. The effect of LiCl on the constitutive as well as virus-induced transcriptional capacity of the IFN-β promoter required the presence of the IFN-β promoter region containing TCF-binding sites, positioned 5' of the VRE region. Results obtained in this work with siRNA directed against β-catenin added to results obtained with iCRT3, an inhibitor of TCF/β-catenin complexes (51) as well as results obtained with IFN-β promoters carrying mutated TCF sites, demonstrated that the capacity of LiCl to enhance IFN-β expression was mediated through TCF/β-catenin complexes rather than IRF3 as suggested until now in the literature.

In the absence of β-catenin, TCFs act as transcriptional repressors recruiting co-repressor complexes. The TCF sites we describe here on the IFNβ promoter are positioned over the NRDII region that corresponds to a negative regulatory region. It is therefore possible that in the absence of β-catenin, TCF factors could be participating in the establishment of the repressive state of the IFN-β promoter alongside with other repressors and co-repressors previously described as participating in the establishment of the repressive state of the IFNβ promoter such as the SAP30/Sin3A/NCoR/HDAC3 complex (21).

Such capacity of LiCl to enhance the transcriptional activity of the IFN-β promoter, we also observed it after treatment of the cells with SB216763 and inhibitor IX, which are two other inhibitors of GSK-3, suggesting that the capacity of LiCl to enhance IFN-β expression observed in this work could be the consequence of the inhibition of GSK-3 that is a target that these three inhibitors have in common. In agreement with our results, activation

539 of IFN-β expression after GSK-3 inhibition by SB216763 has been previously described by
540 several groups in the context of the IFN-β expression induced in response to LPS or polyI:C
541 (39, 61, 62), and a positive effect for β-catenin on IFN-β expression has been reported under
542 different contexts (41, 43, 63).

543 However, inhibition of GSK-3 has also been associated to a negative effect on virus-
544 induced IFN-β expression (44). This was observed in the context of SeV infection and
545 required the SeV-induced secretion of WNT2B and WNT9 ligands that in association with the
546 nuclear accumulation of β-catenin triggered a negative feedback loop to reduce and control an
547 excessive IFN-β response. The SeV-dependent negative effect of GSK-3 inhibition on IFN-β
548 expression was shown to be independent of TCF/β-catenin driven transcription and therefore
549 different from the positive effect of GSK-3 inhibition we have observed here on IFN-β
550 expression. Even though the exact mechanism leading to IFN-β inhibition in the case of SeV
551 infection has remained undetermined, it was suggested to depend on the association of IRF3
552 with β-catenin, affecting the late stage of IRF3 transcriptional activity (44). In our study, the
553 TCF/β-catenin activation of IFN-β expression observed in the presence of LiCl, was observed
554 not only in non-infected cells but also after NDV infection including during the period of the
555 establishment of the post-transcriptional turn-off of the IFN-β gene (Fig. 1 I, 6 and 8 hr p.i.).
556 Differences between our results and those of Baril et al. could be related to the fact that
557 contrary to SeV, NDV infection does not induce WNT signaling as translated by the inability
558 of NDV to induce accumulation of nuclear β-catenin even at late times after infection.

559 WNT ligands lead to the nuclear accumulation of β-catenin through a mechanism
560 different from that of LiCl. While LiCl inhibits the kinase activity of GSK-3 preventing β-
561 catenin degradation, WNT ligands induce the plasma membrane recruitment of GSK-3 and
562 AXIN1, disrupting the cytoplasmic GSK3/AXIN/APC destruction complex of β-catenin.

563 Thus, WNT ligands lead to the accumulation of nuclear β-catenin without affecting the kinase
564 activity of GSK3. Lei et al. (64) have described a positive effect of GSK-3 upon IFN-β
565 expression and response independent of the kinase activity of GSK-3, that required the direct
566 interaction of GSK-3 with TBK1 necessary for the TBK1-dependent activation of IRF3 (64).
567 It is possible that the plasma membrane recruitment of GSK-3 induced by WNT ligands in the
568 context of SeV infection, could interfere with the capacity of GSK-3 to interact with and
569 activate TBK1, therefore diminishing through a feedback loop the pool of phosphorylated
570 active IRF3.

571 Our results showed that the LiCl-dependent activation of the IFN-β expression was
572 correlated with the induction of an effective antiviral response. This in agreement with
573 recently published data describing the capacity of LiCl to inhibit H7N7 influenza A (43) and
574 Porcine Reproductive and Respiratory Syndrome (PRRS) (65) virus replication. Interestingly,
575 both these works show results indicative of a role for TCF/β-catenin complexes on these
576 LiCl-dependent inhibitions of viral infection. Contrary to these and our results, Wang et al.
577 (62) have described a LiCl-dependent attenuation of IFN-β expression and viral infection,
578 through a mechanism independent of LiCl/β-catenin complexes related with the capacity of
579 LiCl to inhibition TBK1. To our knowledge, this is the only work that has described an
580 inhibitory effect of LiCl on TBK1. This is an effect of LiCl that we did not observe under our
581 experimental conditions. Notwithstanding that NDV-induced IFN-β expression relies on the
582 activation of RIG-I and TBK1, we never observed an inhibitory effect of LiCl treatment on
583 the IFN-β expression induced by NDV. Not even under conditions when the positive effect of
584 LiCl was not detected, such as when LiCl was unable to induce accumulation of nuclear β-
585 catenin in AML12 cells (Fig. 2 A-D) or unable to induce β-catenin recruitment as in the case
586 of the WT110 IFN-β promoter (Fig. 3). Differences between our results, as well as results
587 obtained in the context of influenza (43) and PPRS (65) virus, and the work of Wang et al.

588 (62) could result from variations on the state of TBK1 under our respective cellular models.
589 TBK1 is an enzyme whose activity strongly relies on its cellular localization that can be
590 affected by a wide diversity of mechanisms and signaling pathways including not only
591 pathogens but also cell growth and proliferation (66).

592 Further emphasizing the potential role for TCF/β-catenin complexes in the
593 establishment of an efficient innate antiviral response, we show here that LiCl treatment of
594 L929 cells protected these cells against the cytopathic effect of RVFV that we show here to
595 negatively target β-catenin in the liver of infected mice. Viral targeting of the formation of
596 active nuclear β-catenin transcription complexes has been observed in the context of
597 infections with other viruses such as influenza H1N1 virus, Human Cytomegalovirus
598 (HCMV), Venezuelan Equine Encephalitis Virus (VEEV) and HIV-1 (40,67-69). Such
599 tendency of viruses to negatively target β-catenin, is in a agreement with the scenario of a
600 positive role for β-catenin during the establishment of an efficient antiviral response.

601 Several reports in the literature point at physiological roles for constitutive IFN-β
602 expression in the absence of viral infection (33). However, little is known concerning the
603 mechanism(s) capable to directly modulate IFN-β expression in naïve cells except for results
604 obtained with *c-Jun*$^{-/-}$ murine embryonic fibroblasts that identified transcription factor c-Jun
605 as a potential regulator of the constitutive level of IFN-β expression (70). Since inhibition of
606 GSK-3, leading to the formation of nuclear TCF/β-catenin complexes, can be reached not
607 only physiologically through pathways associated with Wnt ligands and Akt phosphorylation
608 but also pharmaceutically, results shown here open the possibility of a wide range of cellular
609 and extra-cellular mechanisms susceptible to modulate the level of IFN-β expression in the
610 absence of infection.

611 If we consider that TCF/β-catenin complexes can directly affect constitutive levels of
612 IFN-β expression in the absence of pathogens as described here, then the existence of cross-

613 talks between β-catenin and IFN-β should also be considered beyond the issue of pathogen
614 infection. For example, the capacity of β-catenin to modulate inflammatory and immune
615 responses (71) could be related to its ability to modulate the expression of IFN-β, which is a
616 major regulator of immunity and inflammatory responses. Also, a cross-talk between β-
617 catenin and IFN-β during the establishment and/or treatment of neurological disorders such as
618 Alzheimer disease and multiple sclerosis should be considered since both Wnt/β-catenin
619 pathway and IFN-β response have been associated to these neurological pathologies (72-74).
620 Although modulation of the constitutive level of IFN-β expression has probably been
621 observed in the past by many researchers, it has often been neglected because it seemed only
622 minor compared to pathogen-induced IFN-β expression. Nevertheless, even though weak, the
623 biological significance of constitutive IFN-β expression is no longer to be demonstrated (33).
624 Therefore, mechanisms capable to modulate constitutive IFN-β expression, such as the one
625 our results demonstrate here, should gain interest in the future.
626
627
628
629
630
631
632
633
634
635
636
637

Acknowledgements. This work was supported by Agence Nationale de la Recherche (ANR) grant ANR-11-BSV3-007 to E.B., M.F. and JJ.P. V. Marcato was financed by the DIM-Malinf project from Région Ile-de-France.

We are grateful to Carole Tamietti for RVFV infections and to Danielle Blondel for gift of the antibody directed against the N protein of VSV.

References

1. **Stark GR, Kerr IM, Williams BR, Silverman RH, Schreiber RD.** 1998. How cells respond to interferons. Annu Rev Biochem **67**:227-64.

2. **Stetson DB, Medzhitov R.** 2006. Type I interferons in host defense. Immunity **25**:373-81.

3. **Jensen S, Thomsen AR.** 2012. Sensing of RNA viruses: a review of innate immune receptors involved in recognizing RNA virus invasion. J Virol **86**:2900-10

4. **Randall RE, Goodbourn S.** 2008. Interferons and viruses: an interplay between induction, signalling, antiviral responses and virus countermeasures. J Gen Virol **89**:1-47.

5. **Deonarain R, Alcamí A, Alexiou M, Dallman MJ, Gewert DR, Porter AC.** 2000. Impaired antiviral response and alpha/beta interferon induction in mice lacking beta interferon. J Virol **74**:3404-9.

6. **Müller U, Steinhoff U, Reis LF, Hemmi S, Pavlovic J, Zinkernagel RM, Aguet M.** 1994. Functional role of type I and type II interferons in antiviral defense. Science **264**:1918-21.

7. **Hwang SY, Hertzog PJ, Holland KA, Sumarsono SH, Tymms MJ, Hamilton JA, Whitty G, Bertoncello I, Kola I.** 1995. A null mutation in the gene encoding a type I interferon receptor component eliminates antiproliferative and antiviral responses to interferons alpha and beta and alters macrophage responses. Proc Natl Acad Sci USA **92**:11284-8.

8. **Hall JC, Rosen A.** 2010. Type I interferons: crucial participants in disease amplification in autoimmunity. Nat. Rev. Rheumatol. **6**:40-9.

9. **Crow MK.** 2010. Type I interferon in organ-targeted autoimmune and inflammatory diseases. Arthritis Res Ther **12**(Suppl 1):S5.

669 10. **Choubey D, Moudgil KD.** 2011. Interferons in autoimmune and inflammatory diseases:
670 regulation and roles. J Interferon Cytokine Res **31**:857-65.
671 11. **Trinchieri G.** 2010. Type I interferon: friend or foe? J Exp Med **207**:2053-63.
672 12. **Prinz M, Knobeloch KP.** 2012. Type I interferons as ambiguous modulators of chronic
673 inflammation in the central nervous system. Front Immunol **3**:67.
674 13. **Hu J, Sealfon SC, Hayot F, Jayaprakash C, Kumar M, Pendleton AC, Ganee A,**
675 **Fernandez-Sesma A, Moran TM, Wetmur JG.** 2007. Chromosome-specific and noisy
676 IFNB1 transcription in individual virus-infected human primary dendritic cells. Nucleic Acids
677 Res **35**:5232-41.
678 14. **Zhao M, Zhang J, Phatnani H, Scheu S, Maniatis T.** 2012. Stochastic expression of the
679 interferon-β gene. PLoS Biol **10**:e1001249.
680 15. **Apostolou E, Thanos D.** 2008. Virus Infection Induces NF-kappaB-dependent
681 interchromosomal associations mediating monoallelic IFN-beta gene expression. Cell **134**:85-
682 96.
683 16. **Josse T, Mokrani-Benhelli H, Benferhat R, Shestakova E, Mansuroglu Z,**
684 **Kakanakou H, Billecocq A, Bouloy M, Bonnefoy E.** 2012. Association of the interferon-β
685 gene with pericentromeric heterochromatin is dynamically regulated during virus infection
686 through a YY1-dependent mechanism. Nucleic Acids Res **40**:4396-411.
687 17. **Maniatis T, Falvo JV, Kim TH, Kim TK, Lin CH, Parekh BS, Wathelet MG.** 1998.
688 Structure and function of the interferon-beta enhanceosome. Cold Spring Harb Symp Quant
689 Biol **63**:609-20.
690 18. **Agalioti T, Lomvardas S, Parekh B, Yie J, Maniatis T, Thanos D.** 2000. Ordered
691 recruitment of chromatin modifying and general transcription factors to the IFN-beta
692 promoter. Cell **103**:667-78.

693 19. **Agalioti T, Chen G, Thanos D.** 2002. Deciphering the transcriptional histone acetylation
694 code for a human gene. Cell **111**:381-92.
695 20. **Mokrani H, Sharaf el Dein O, Mansuroglu Z, Bonnefoy E.** 2006. Binding of YY1 to
696 the proximal region of the murine beta interferon promoter is essential to allow CBP
697 recruitment and K8H4/K14H3 acetylation on the promoter region after virus infection. Mol
698 Cell Biol **26**:8551-61.
699 21. **Le May N, Mansuroglu Z, Léger P, Josse T, Blot G, Billecocq A, Flick R, Jacob Y,**
700 **Bonnefoy E, Bouloy M.** 2008. A SAP30 complex inhibits IFN-beta expression in Rift Valley
701 fever virus infected cells. PLoS Pathog **4**:e13.
702 22. **Sato M, Taniguchi T, Tanaka N.** 2001. The interferon system and interferon regulatory
703 factor transcription factors -- studies from gene knockout mice. Cytokine Growth Factor Rev
704 **12**:133-42.
705 23. **Kim TK, Kim TH, Maniatis T.** 1998. Efficient recruitment of TFIIB and CBP-RNA
706 polymerase II holoenzyme by an interferon-beta enhanceosome in vitro. Proc Natl Acad Sci U
707 S A **95**:12191-6.
708 24. **Panne D, Maniatis T, Harrison SC.** 2004. Crystal structure of ATF-2/c-Jun and IRF-3
709 bound to the interferon-beta enhancer. EMBO J **23**:4384-93.
710 25. **Klar M, Bode J.** 2005. Enhanceosome formation over the beta interferon promoter
711 underlies a remote-control mechanism mediated by YY1 and YY2. Mol Cell Biol **25**:10159-
712 70.
713 26. **Siednienko J, Maratha A, Yang S, Mitkiewicz M, Miggin SM, Moynagh PN.** 2011.
714 Nuclear factor κB subunits RelB and cRel negatively regulate Toll-like receptor 3-mediated
715 β-interferon production via induction of transcriptional repressor protein YY1. J Biol Chem
716 **286**:44750-63.

717 27. **Weill L, Shestakova E, Bonnefoy E.** 2003. Transcription factor YY1 binds to the murine
718 beta interferon promoter and regulates its transcriptional capacity with a dual
719 activator/repressor role. J Virol **77**:2903-14.
720 28. **Dafny N, Yang PB.** 2005. Interferon and the central nervous system. Eur J Pharmacol
721 **523**:1-15.
722 29. **Prinz M, Schmidt H, Mildner A, Knobeloch KP, Hanisch UK, Raasch J, Merkler D,**
723 **Detje C, Gutcher I, Mages J, Lang R, Martin R, Gold R, Becher B, Brück W, Kalinke U.**
724 2008. Distinct and nonredundant in vivo functions of IFNAR on myeloid cells limit
725 autoimmunity in the central nervous system. Immunity **28**:675-86.
726 30. **Hata N, Sato M, Takaoka A, Asagiri M, Tanaka N, Taniguchi T.** 2001. Constitutive
727 IFN-alpha/beta signal for efficient IFN-alpha/beta gene induction by virus. Biochem Biophys
728 Res Commun **285**:518-25.
729 31. **Haller O, Arnheiter H, Gresser I, Lindenmann J.** 1979. Genetically determined,
730 interferon-dependent resistance to influenza virus in mice. J Exp Med **149**:601-12.
731 32. **Vogel SN, Fertsch D.** 1984. Endogenous interferon production by endotoxin-responsive
732 macrophages provides an autostimulatory differentiation signal. Infect Immun **45**:417-23.
733 33. **Gough DJ, Messina NL, Clarke CJ, Johnstone RW, Levy DE.** 2012. Constitutive type
734 I interferon modulates homeostatic balance through tonic signaling. Immunity **36**:166-74.
735 34. **MacDonald BT, Tamai K, He X.** 2009. Wnt/beta-catenin signaling: components,
736 mechanisms, and diseases. Dev Cell **17**:9-26.
737 35. **Valenta T, Hausmann G, Basler K.** 2012. The many faces and functions of β-catenin.
738 EMBO J **31**:2714-36.
739 36. **Sampietro J, Dahlberg CL, Cho US, Hinds TR, Kimelman D, Xu W.** 2006. Crystal
740 structure of a beta-catenin/BCL9/Tcf4 complex. Mol Cell **24**:293-300.

741 37. **Deka J, Wiedemann N, Anderle P, Murphy-Seiler F, Bultinck J, Eyckerman S,**
742 **Stehle JC, André S, Vilain N, Zilian O, Robine S, Delorenzi M, Basler K, Aguet M.** 2010.
743 Bcl9/Bcl9l are critical for Wnt-mediated regulation of stem cell traits in colon epithelium and
744 adenocarcinomas. Cancer Res **70**:6619-28.
745 38. **Archbold HC, Yang YX, Chen L, Cadigan KM.** 2011. How do they do Wnt they do?:
746 regulation of transcription by the Wnt/β-catenin pathway. Acta Physiol (Oxf) **204**:74-109.
747 39. **Wang H, Garcia CA, Rehani K, Cekic C, Alard P, Kinane DF, Mitchell T, Martin M.**
748 2008. IFN-beta production by TLR4-stimulated innate immune cells is negatively regulated
749 by GSK3-beta. J Immunol **181**:6797-802.
750 40. **Shapira SD, Gat-Viks I, Shum BO, Dricot A, de Grace MM, Wu L, Gupta PB, Hao**
751 **T, Silver SJ, Root DE, Hill DE, Regev A, Hacohen N.** 2009. A physical and regulatory map
752 of host-influenza interactions reveals pathways in H1N1 infection. Cell **139**:1255-67.
753 41. **Yang P, An H, Liu X, Wen M, Zheng Y, Rui Y, Cao X.** 2010. The cytosolic nucleic
754 acid sensor LRRFIP1 mediates the production of type I interferon via a beta-catenin-
755 dependent pathway. Nat Immunol **11**:487-94.
756 42. **Zhu J, Coyne CB, Sarkar SN.** 2011. PKC alpha regulates Sendai virus-mediated
757 interferon induction through HDAC6 and β-catenin. EMBO J **30**:4838-49.
758 43. **Hillesheim A, Nordhoff C, Boergeling Y, Ludwig S, Wixler V.** 2014. β-catenin
759 promotes the type I IFN synthesis and the IFN-dependent signaling response but is suppressed
760 by influenza A virus-induced RIG-I/NF-κB signaling. Cell Commun Signal **12**:29.
761 44. **Baril M, Es-Saad S, Chatel-Chaix L, Fink K, Pham T, Raymond VA, Audette K,**
762 **Guenier AS, Duchaine J, Servant M, Bilodeau M, Cohen E, Grandvaux N, Lamarre D.**
763 2013. Genome-wide RNAi screen reveals a new role of a WNT/CTNNB1 signaling pathway
764 as negative regulator of virus-induced innate immune responses. PLoS Pathog **9**:e1003416.

765 45. **Bonnefoy E, Bandu MT, Doly J.** 1999. Specific binding of high-mobility-group I
766 (HMGI) protein and histone H1 to the upstream AT-rich region of the murine beta interferon
767 promoter: HMGI protein acts as a potential antirepressor of the promoter. Mol Cell Biol
768 **19**:2803-16.
769 46. **Gommet C, Billecocq A, Jouvion G, Hasan M, Zaverucha do Valle T, Guillemot L,**
770 **Blanchet C, van Rooijen N, Montagutelli X, Bouloy M, Panthier JJ.** 2011. Tissue tropism
771 and target cells of NSs-deleted rift valley fever virus in live immunodeficient mice. PLoS
772 Negl Trop Dis **5**:e1421.
773 47. **Yadani FZ, Kohl A, Préhaud C, Billecocq A, Bouloy M.** 1999. The carboxy-terminal
774 acidic domain of Rift Valley Fever virus NSs protein is essential for the formation of
775 filamentous structures but not for the nuclear localization of the protein. J Virol **73**:5018-25.
776 48. **Taniguchi T, Takaoka A.** 2001. A weak signal for strong responses: interferon-
777 alpha/beta revisited. Nat Rev Mol Cell Biol **2**:378-86.
778 49. **Solomon MJ, Strauss F, Varshavsky A.** 1986. A mammalian high mobility group
779 protein recognizes any stretch of six A.T base pairs in duplex DNA. Proc Natl Acad Sci USA
780 **83**:1276-80.
781 50. **van de Wetering M, Clevers H.** 1992. Sequence-specific interaction of the HMG box
782 proteins TCF-1 and SRY occurs within the minor groove of a Watson-Crick double helix.
783 EMBO J **8**:3039-44.
784 51. **Gonsalves FC, Klein K, Carson BB, Katz S, Ekas LA, Evans S, Nagourney R,**
785 **Cardozo T, Brown AM, DasGupta R.** 2011. An RNAi-based chemical screen identifies
786 three small-molecule inhibitors of the Wnt/*wingless* signaling pathway. Proc Natl Acad Sci
787 USA **108**:5954-63.

52. **Shestakova E, Bandu MT, Doly J, Bonnefoy E.** 2001. Inhibition of histone deacetylation induces constitutive derepression of the beta interferon promoter and confers antiviral activity. J Virol **75**:3444-52.

53. **Pepin M, Bouloy M, Bird BH, Kemp A, Paweska J.** 2010. Rift Valley fever virus(Bunyaviridae: Phlebovirus): an update on pathogenesis, molecular epidemiology, vectors, diagnostics and prevention. Vet Res **6**:61.

54. **do Valle TZ, Billecocq A, Guillemot L, Alberts R, Gommet C, Geffers R, Calabrese K, Schughart K, Bouloy M, Montagutelli X, Panthier JJ.** 2010. A new mouse model reveals a critical role for host innate immunity in resistance to Rift Valley fever. J Immunol **185**:6146-56.

55. **Ikegami T.** 2012. Molecular biology and genetic diversity of Rift Valley fever virus. Antiviral Res. **95**:293-310.

56. **Billecocq A, Gauliard N, Le May N, Elliott RM, Flick R, Bouloy M.** 2008. RNA polymerase I-mediated expression of viral RNA for the rescue of infectious virulent and avirulent Rift Valley fever viruses. Virology **378**:377-84.

57. **Le May N, Dubaele S, Proietti De Santis L, Billecocq A, Bouloy M, Egly JM.** 2004. TFIIH transcription factor, a target for the Rift Valley hemorrhagic fever virus. Cell **116**:541-50.

58. **Benferhat R, Josse T, Albaud B, Gentien D, Mansuroglu Z, Marcato V, Souès S, Le Bonniec B, Bouloy M, Bonnefoy E.** 2012. Large-scale chromatin immunoprecipitation with promoter sequence microarray analysis of the interaction of the NSs protein of Rift Valley fever virus with regulatory DNA regions of the host genome. J Virol **86**:11333-44.

59. **Jho EH, Zhang T, Domon C, Joo CK, Freund JN, Costantini F.** 2002. Wnt/beta-catenin/Tcf signaling induces the transcription of Axin2, a negative regulator of the signaling pathway. Mol Cell Biol **22**:1172-83.

60. **Reed C, Steele KE, Honko A, Shamblin J, Hensley LE, Smith DR.** 2012. Ultrastructural study of Rift Valley fever virus in the mouse model. Virology **431**:58-70.

61. **Gantner BN, Jin H, Qian F, Hay N, He B, Ye RD.** 2012. The Akt1 isoform is required for optimal IFN-β transcription through direct phosphorylation of β-catenin. J Immunol **189**:3104-11.

62. **Wang L, Zhang L, Zhao X, Zhang M, Zhao W, Gao C.** 2013. Lithium attenuates IFN-β production and antiviral response via inhibition of TANK-Binding Kinase 1 kinase activity. J Immunol **191**:4392-8.

63. **Ma F, Liu SY, Razani B, Arora N, Li B, Kagechika H, Tontonoz P, Núñez V, Ricote M, Cheng G.** 2014. Retinoid X receptor α attenuates host antiviral response by suppressing type I interferon. Nat Commun **5**:5494.

64. **Lei CQ, Zhong B, Zhang Y, Zhang J, Wang S, Shu HB.** 2010. Glycogen synthase kinase 3β regulates IRF3 transcription factor-mediated antiviral response via activation of the kinase TBK1. Immunity **33**:878-89.

65. **Hao HP, Wen LB, Li JR, Wang Y, Ni B, Wang R, Wang X, Sun MX, Fan HJ, Mao X.** 2015. LiCl inhibits PRRSV infection by enhancing Wnt/β-catenin pathway and suppressing inflammatory responses. Antiviral Res 117 :99-109.

66. **Helgason E, Phung QT, Dueber EC.** 2013. Recent insights into the complexity of Tank-binding kinase 1 signaling networks: the emerging role of cellular localization in the activation and substrate specificity of TBK1. FEBS Lett **587**:1230-7.

67. **Angelova M, Zwezdaryk K, Ferris M, Shan B, Morris CA, Sullivan DE.** 2012. Human cytomegalovirus infection dysregulates the canonical Wnt/β-catenin signaling pathway. PLoS Pathog **8**:e1002959.

68. **Kehn-Hall K, Narayanan A, Lundberg L, Sampey G, Pinkham C, Guendel I, Van Duyne R, Senina S, Schultz KL, Stavale E, Aman MJ, Bailey C, Kashanchi F.** 2012.

838 Modulation of GSK-3β activity in Venezuelan equine encephalitis virus infection. PLoS One
839 **7**:e34761.
840 69. **Henderson LJ, Sharma A, Monaco MC, Major EO, Al-Harthi L.** 2012. Human
841 immunodeficiency virus type 1 (HIV-1) transactivator of transcription through its intact core
842 and cysteine-rich domains inhibits Wnt/β-catenin signaling in astrocytes: relevance to HIV
843 neuropathogenesis. J Neurosci **32**:16306-13.
844 70. **Gough DJ, Messina NL, Hii L, Gould JA, Sabapathy K, Robertson AP, Trapani JA,**
845 **Levy DE, Hertzog PJ, Clarke CJ, Johnstone RW.** 2010. Functional crosstalk between type
846 I and II interferon through the regulated expression of STAT1. PLoS Biol **8**:e1000361.
847 71**. Manicassamy S, Reizis B, Ravindran R, Nakaya H, Salazar-Gonzalez RM, Wang**
848 **YC, Pulendran B.** 2010. Activation of beta-catenin in dendritic cells regulates immunity
849 versus tolerance in the intestine. Science **329**:849-53.
850 72. **Taylor JM, Minter MR, Newman AG, Zhang M, Adlard PA, Crack PJ.** 2013. Type-1
851 interferon signaling mediates neuro-inflammatory events in models of Alzheimer's disease.
852 Neurobiol. Aging **35**:1012-23.
853 73. **Xie C, Li Z, Zhang GX, Guan Y.** 2013. Wnt Signaling in Remyelination in Multiple
854 Sclerosis: Friend or Foe? Mol Neurobiol **49**:1117-25.
855 74. **Rosso SB, Inestrosa NC.** 2013. WNT signaling in neuronal maturation and
856 synaptogenesis. Front Cell Neurosci **7**:103.
857

858 **Figure legends**

859 **Figure 1. LiCl treatment enhances the constitutive and virus-induced IFN-β expression.**
860 **(A)** Schematic representation of the general organization of the murine IFN-β promoter
861 showing the Negative Regulatory Domain (NRD) I and II as well as the Virus Responsive
862 Element (VRE). (**B** and **H**) Immunolocalisation of β-catenin in L929. Cells were either non-
863 treated (NT), treated with 20mM LiCl (LiCl) during 24h, or infected with NDV, labeled with
864 an anti-β-catenin antibody (a, d, g, h) and a DNA intercalating agent to visualize the nucleus
865 (ToPro3; b, e, h, k). Nuclei were outlined as shown in merge images and total green pixel
866 intensity corresponding to β-catenin labeling in the nucleus was quantified **(C).** β-catenin was
867 analyzed by Western blot (**D**) in nuclear extracts from L929 cells either non treated (NT) or
868 treated with 20 mM LiCl (LiCl) during 24h. IFN-β mRNA (**E** and **I**) and Oas1b or IRF7
869 mRNA (**F**) were analyzed by RT-qPCR: in non-infected L929 cells either non-treated (NT) or
870 LiCl treated (LiCl) (**E-G**); at different times post-infection (p.i) in L929 cells mock- or NDV-
871 infected, either non-treated (NT) or pre-treated with LiCl (LiCl) (**I**). In (**E-G**), the
872 corresponding fold inductions were calculated with respect to non treated cells; and in (**I**), the
873 corresponding fold inductions were calculated with respect to non-infected and non-treated
874 cells. **C**) n=33 (minimum) to 71 (maximum) counted nuclei; **E**) n=42 from 13 independent
875 experiences; **F**) n=18 from 6 independent experiences; **I**) n=6. Student test: p-value less than
876 0.001 (***), 0.01 (**) and 0.05 (*). All images correspond to one confocal section. Scale bar
877 = 10μM.
878
879 **Figure 2. LiCl enhancement of IFN-β expression is mediated by β-catenin.** (**A-D**) AML12
880 cells were either non-treated (NT) or treated with 20mM LiCl (LiCl) during 24h and either
881 non-infected (**A-C**) or NDV-infected (**D**). (**A** and **B**) Cells were labeled with an anti-β-catenin
882 antibody (a, d) and a DNA intercalating agent to visualize the nucleus (ToPro3; b, e). Nuclei

were outlined as shown in merge images (c, f), and total green pixel intensity corresponding to β-catenin labeling in the nucleus was quantified (**B**). IFN-β mRNA (**C** and **D**) was analyzed by RT-qPCR in non-infected (**C**) and NDV-infected (6h p.i.) (**D**) cells either non-treated (NT) or pre-treated with LiCl (LiCl). The corresponding fold inductions were calculated with respect to non-treated (**C**) or non-infected and non-treated (**D**) cells. (**E-G**) L929 cells were either mock-transfected (mock) or transfected with β-catenin specific (siβcat) or control (siCtrl) siRNA for 72h. β-catenin mRNA (**E**) and protein level (**F**) were analyzed by RT-qPCR and WB respectively. (**G**) Post-siRNA, cells were either non-treated (NT) or treated with 20mM LiCl (LiCl) during 24h before being NDV-infected. IFN-β mRNA was analyzed by RT-qPCR. (**E** and **G**) the corresponding fold inductions were calculated with respect to mock-transfected, non-treated and NDV-infected cells (n=3). Student test: p-value less than 0.001 (***) and 0.01 (**). All images correspond to one confocal section. Scale bar = 10μM.

Figure 3. Interaction of β-catenin with the IFN-β promoter region containing a TCF binding site is necessary for LiCl enhancement of IFN-β promoter activity. (A) Schematic representation of the WT330 and WT110 murine IFN-β promoters fused to the CAT reporter gene and integrated into the genome of L929 WT330 and L929 WT110 cell lines respectively. **(B** to **D)** β-catenin binding to WT330 and WT110 promoters and corresponding CAT activities were analysed in L929 WT330 and WT110 cells either non-treated (NT) or treated with LiCl 20mM (LiCl). **(B)** Genomic DNA was collected 24h post-LiCl treatment and immunoprecipited with anti β-catenin (α-β-cat) or anti NSs (α-NSs, negative control) antibodies. Increasing amounts (μL) of immunuprecipitated DNA (IP), as well as non immunoprecipitated genomic DNA (Input) were amplified by semi-quantitative PCR using specific primers for the WT330 and WT110 integrated promoters. **(C)** Cells were

907 collected post-LiCl treatment and their CAT activities quantified. The corresponding fold
908 inductions were calculated with respect to non-treated cells (n=12 for WT330 and n=6 for
909 WT110 cell lines). **(D)** Post-LiCl treatment, cells were further mock- or NDV-infected,
910 collected at different times post-infection and the corresponding CAT activities were
911 quantified. The corresponding fold inductions were calculated with respect to non-infected
912 non-treated cells (n=4). **(E and F)** CAT activities of L929 cells either non-treated (NT) or
913 treated with 50 μM of SB216763 (**E**) or 30μM of IX inhibitor during 24h (**F**). Cells were
914 further mock- or NDV-infected, collected 8h post-infection and the corresponding CAT
915 activities quantified. The corresponding fold inductions were calculated with respect to non-
916 infected non-treated cells.
917
918 **Figure 4. TCF binding sites mediate LiCl-dependent activation of the IFN-β promoter.**
919 (**A** and **B**) Equal amounts of nuclear extracts (N.E) prepared from L929 either non-treated (-
920 LiCl) or treated with 20mM LiCl (+LiCl) during 24h were incubated with the radioactively
921 labeled probes corresponding to wild type TCFa (TCFA) and TCFb (TCFB) or mutated TCFa
922 (TCFmutA) and TCFb (TCFmutB) sites. When indicated, nuclear extracts were incubated
923 with 500 ng of poly dI/dC or anti-β-catenin antibodies before adding the probes. (**C**) L929
924 cells transfected with plasmids containing luciferase reporter gene under the control of the
925 IFN-β promoter either WT or mutated at the TCFa site (mutA), the TCFb site (mutB) or the
926 TCFa and b sites (mutAB) were either non-treated (NT) or pre-treated with LiCl (LiCl) before
927 infection with NDV. Cells were collected 7h p.i. and the luminescence was quantified with
928 n=3. (**D** and **E**) L929 cells were either non-treated (NT) or treated with 20mM LiCl (LiCl)
929 during 24h or 48h in the presence or absence of iCRT3 before being NDV-infected. IFN-β
930 (**D**) or cyclin D1 (**E**) mRNA was analyzed by RT-qPCR and the corresponding fold

inductions were calculated with respect to non-treated NDV-infected (**D**) or non-infected (**E**) cells; **D**) n=3. Student test: p-value less than 0.01 (**) and 0.05 (*).

Figure 5. LiCl treatment confers an antiviral state. Monolayers of L929 cells either non-treated (NT) or pre-treated with LiCl 20mM for 24h were infected with VSV. (**A**) Cytopathic effect induced by increasing MOI of VSV was assayed by crystal violet dye staining 24h after infection; (**B**) Photographs of typical culture fields. (**C** and **D**) Cells were fixed 8h after infection (MOI=1), labeled with an antibody directed against the N protein of VSV (displayed in gray) and ToPro3 (blue); merge images of the corresponding culture fields are displayed in (**C**). The % of infected cells, as determined by the presence of N protein encoded by VSV (fluorescence displayed in gray) was determined from a total of 7876 untreated and 9024 LiCl-treated cells counted with n=4 (**D**).

Figure 6. Infection with RVFV affects the Wnt/β-catenin pathway at the transcriptional level. The expression of genes associated to the Wnt/β-catenin pathway previously identified as interacting with the NSs protein of RVFV (listed in Table II) was measured in three different cell types corresponding to fibroblast (L929), hepatocytes (AML12) and Bone Marrow Derived Macrophages (BMDM) either mock-, RVFZH548- (ZH) or RVFVΔNSs- (ΔNSs) infected. RNAs purified from mock- or virus-infected cells (8h p.i.) were analyzed by RT-qPCR with primers specific for each gene of interest. The change in gene expression was calculated in ZH and ΔNSs-infected cells with respect to mock-infected cells. The horizontal broken lines indicate the cutoff value for upregulation (+1.5 fold) and downregulation (-1.5 fold). The effect of virus infection upon the expression of genes coding for WNT ligands as well as for antagonist of Wnt signaling (*Apcdd1*, *Dkk1* and *Kremen2*) could not be tested since the corresponding mRNA remained undetectable in the three cell types analyzed here. n≥3 for each cell line.

Figure 7. Non-pathogenic and pathogenic strains of RVFV have opposite effects on the Wnt/β-catenin pathway. Genes participating in the Wnt/β-catenin pathway whose promoter regions were identified as significantly interacting with RVFV NSs protein during ChIP-on-chip experiments, listed in Table II, are shown in gray. Genes whose expressions were affected after infection with either the non-pathogenic ΔNSs or the pathogenic ZH strain of RVFV with respect to mock-infected cells are indicated by blue (upregulated) or red (downregulated) arrows.

Figure 8. A physiological relevance for β-catenin protein level during RVFV infection. **(A** and **B)** β-catenin protein and viral N and NSs RNA levels were evaluated in liver and brain of mice either non-infected (NI) or at days 3 and 5 p.i. with RVFVZH548 (ZH) or RVFVΔNSs (ΔNSs). **(A)** β-catenin protein level was analysed by Western blot and estimated densitometrically by comparison with the band intensity of GAPDH; values were averaged from (n) independent samples per time point with n=3 mice (NI), n=6 mice (ZH 3 days and ΔNSs 3 and 5 days) and n=4 mice (ZH 5 days). Fold induction was calculated by comparison of the relative β-catenin level in infected versus non-infected (NI) samples. **(B)** The relative level of viral N and NSs mRNA were estimated by comparison with the expression of three reference genes (Ppib, Hprt1 and Utp6c). (**C**) Number of lytic plaques formed in monolayers of L929 cells either non treated or pre-treated with LiCl 20 mM during 24h and infected with RVFVZH548. Cells were fixed and stained with crystal violet 3 days p.i. (n=4). Student test: p-value less than 0.001 (***), 0.01 (**) and 0.05 (*). All images correspond to one confocal section.

980 **Table I.** Sequences of the different primers used during qPCR assays.

	Forward	Reverse
Ppib	GGAGATGGCACAGGAGGAAA	CCGTAGTGCTTCAGTTTGAAGTTCT
Hprt1	TCCTCCTCAGACCGCTTTT	CCTGGTTCATCATCGCTAATC
Utp6c	TTTCGGTTGAGTTTTTCAGGA	CCCTCAGGTTTACCATCTTGC
Rplp0	CACTGGTCTAGGACCCGAGAAG	GGTGCCTCTGGAGATTTTCG
Ifnb1	ATGAACAACAGGTGGATCCTCC	AGGAGCTCCTGACATTTCCGAA
Os1b	GAGGTGCCGACGGAGGT	TCCAGATGAAGTCTTCCCAAAG
IRF7	CAGCGAGTGCTGTTTGGAGAC	AAGTTCGTACACCTTATGCGG
Ctnnb1	GCCACAGGATTACAAGAAGC	CCACCAGAGTGAAAAGAACG
Bcl9	AGTGCTCTCTCCAGGATATGATG	GGGCAAAGAGTGTGAAATGTTG
Csnk1d	ACGCCGGGATCGAGAAGAA	CCGACCGGGAATCTGTGAG
Csnk1g2	CAAACTTCCGAGTCGGCAAGA	GCTTGTAAAAGCGGTACTCCAG
Csnk1g3	TGGGACCGAGTTTGGAGGATT	CTGGCCGTCCTATTAAGAAGTTC
Csnk2a2	TCCCGAGCTGGGGTAATCAA	TGTTCCACCACGAAGGTTCTC
Tcf7l2	CACGACAGGAGGATTCAGA	GGGGCTTCTTCTTCTCTTC
Axin2	TGACTCTCCTTCCAGATCCCA	TGCCCACACTAGGCTGACA
Gsk3b	TGGCAGCAAGGTAACCACAG	CGGTTCTTAAATCGCTTGTCCTG

981

Table II. List of canonical Wnt/β-catenin genes whose regulatory DNA regions were identified as interacting with RVFV NSs protein during ChIP-on-chip assays (55).

Gene	Chromo-some	NSs interacting Region Start	Region Length (bps)	Probes in Region	p-value
Apcdd1	Chr18	63078268	563	16	0.007658
Axin2	Chr11	108827835	502	14	0.00618531
Bcl9	Chr3	97004948	751	21	0.00823024
Csnk1d	Chr11	120859171	651	18	0.0033914
Csnk1g2	Chr10	80096623	865	24	0.00136329
Csnk1g2	Chr10	80082196	920	22	0.00671548
Csnk1g3	Chr18	54109583	850	18	0.00104351
Csnk1g3	Chr18	54156237	499	10	0.00828074
Csnk2a2	Chr8	97965333	511	12	0.00827232
Ctnnb1	Chr9	120803511	517	15	0.00766641
Gsk3a	Chr7	26016588	488	14	0.00998065
Gsk3b	Chr16	38213326	554	16	0.006564
Kremen2	Chr17	23882003	542	14	0.00559623
Lef1	Chr3	130837713	488	13	0.00916435
Tcf7l2	Chr19	55894582	531	15	0.00931583
Wnt1	Chr15	98620114	407	11	0.00822183
Wnt2	Chr6	17981380	579	17	0.00595809
Wnt6	Chr1	74823318	824	23	0.00226374
Wnt6	Chr1	74830849	550	14	0.00750652
Wnt6	Chr1	74828942	494	14	0.00782631
Wnt6	Chr1	74818891	394	11	0.00812085
Wnt6	Chr1	74816494	489	13	0.00885298
Wnt8b	Chr19	44545480	754	20	0.00226374
Wnt8b	Chr19	44544618	808	23	0.00506606

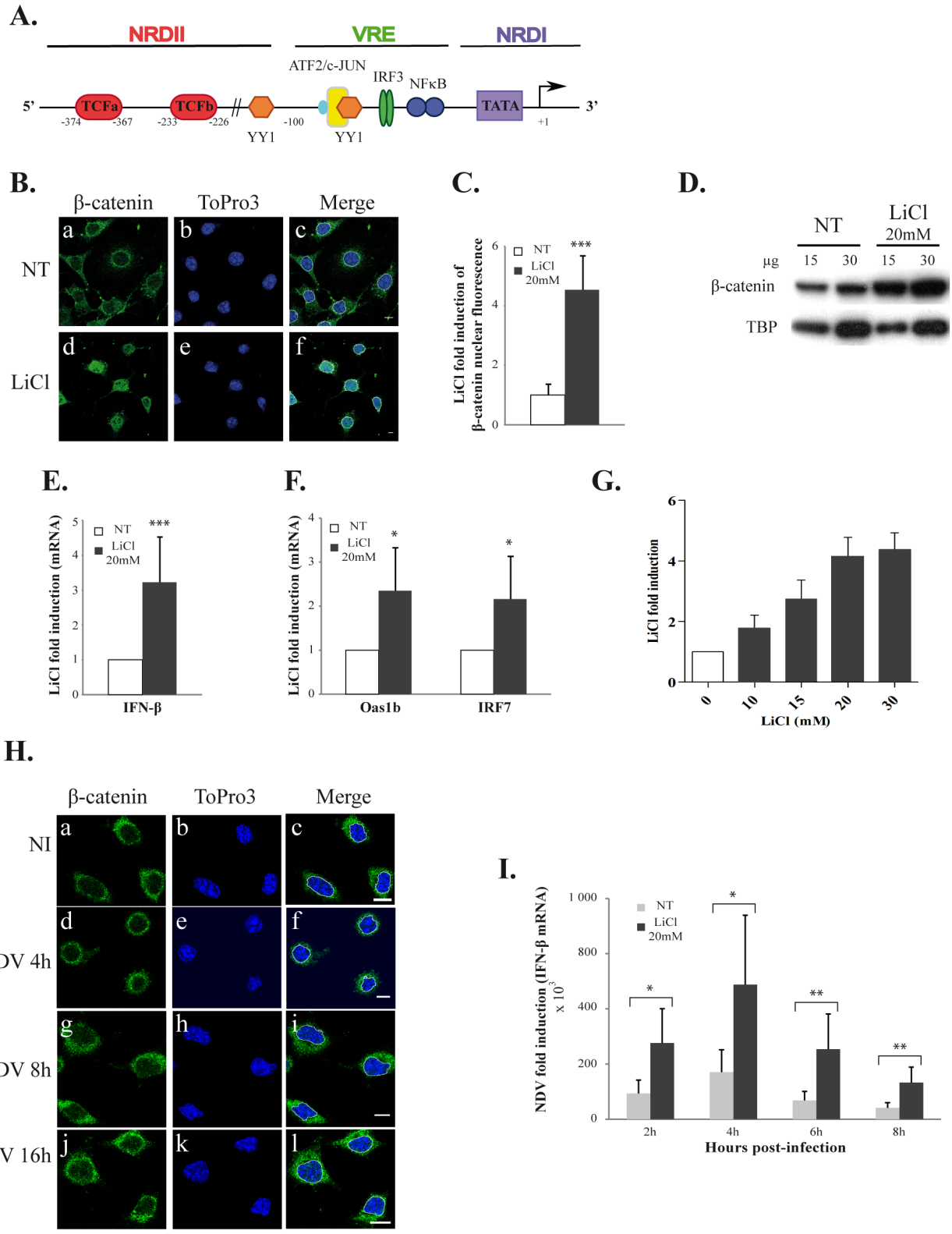

Figure 1. **LiCl treatement enhances the constitutive and virus-induced IFN-β expression**. (**A**) Schematic representation of the general organization of the murine IFN-β promoter showing the Negative Regulatory Domain (NRD) I and II as well as the Virus Responsive Element (VRE). (**B** and **H**) Immunolocalisation of β-catenin in L929 cells. Cells were either non-treated (NT), treated with 20mM LiCl (LiCl) during 24h, non infected (NI) or infected with NDV, labeled with an anti-β-catenin antibody (a,d,g,j) and a DNA intercalating agent to visualize the nucleus (ToPro3; b,e,h,k). Nuclei were outlined as shown in merge images, and total green pixel intensity corresponding to β-catenin labeling in the nucleus was quantified (**C**) . β-catenin protein level was analyzed by Western Blot (**D**) in nuclear extracts from L929 cells either non treated (NT) or treated with 20mM LiCl (LiCl) during 24h. IFN-β mRNA (**E** and **I**) and Oas1b or IRF7 mRNA (**F**) were analyzed by RT-qPCR: in non-infected L929 cells either non-treated (NT) or LiCl treated (LiCl) (**E** - **G**); at different times post-infection (p.i) in L929 cells mock- or NDV-infected, either non-treated (NT) or pre-treated with LiCl (LiCl) (**I**). In (**E** - **G**), the corresponding fold inductions were calculated with respect to non-treated cells; and in (**I**), the corresponding fold inductions were calculated with respect to non-infected and non-treated cells. **C**) n=33 (minimum) to 71 (maximum) counted nuclei; **E**) n=42 from 13 independent experiences; **F**) n=18 from 6 independent experiences; **I**) n=6. Student test: p-value less than 0.001 (***), 0.01 (**) and 0.05 (*). All images correspond to one confocal section. Scale bar = 10µM.

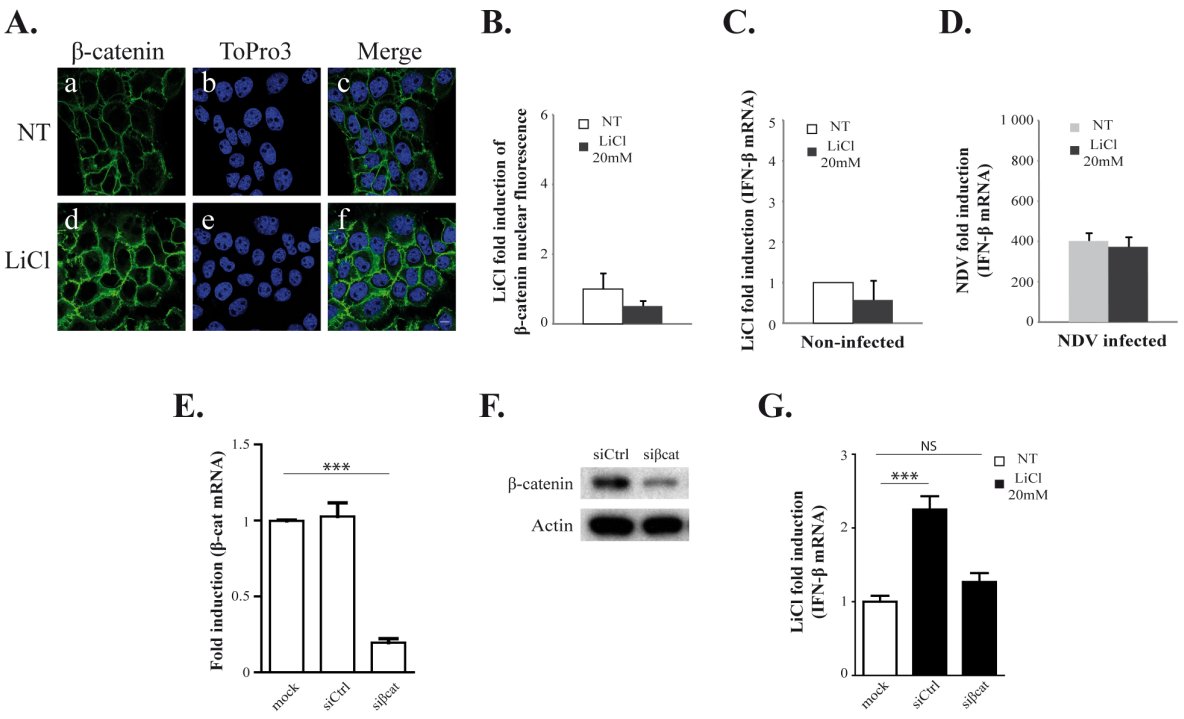

Figure 2. LiCl enhancement of IFN-β expression is mediated by β-catenin. (**A**-**D**) AML12 cells were either non-treated (NT) or treated with 20mM LiCl (LiCl) during 24h and either non-infected (**A**-**C**) or NDV-infected (**D**). (**A** and **B**) Cells were labeled with an anti-β-catenin antibody (a, d) and a DNA intercalating agent to visualize the nucleus (ToPro3; b, e). Nuclei were outlined as shown in merge images (c, f), and total green pixel intensity corresponding to β-catenin labeling in the nucleus was quantified (**B**). IFN-β mRNA (**C** and **D**) was analyzed by RT-qPCR in non-infected (**C**) and NDV-infected (6h p.i.) (**D**) cells either non-treated (NT) or pre-treated with LiCl (LiCl). The corresponding fold inductions were calculated with respect to non-treated (**C**) or non-infected and non-treated (**D**) cells. (**E**-**G**) L929 cells were either mock-transfected (mock) or transfected with β-catenin specific (siβcat) or control (siCtrl) siRNA for 72h. β-catenin mRNA (**E**) and protein level (**F**) were analyzed by RT-qPCR and WB respectively. (**G**) Post-siRNA, cells were either non-treated (NT) or treated with 20mM LiCl (LiCl) during 24h before being NDV-infected. IFN-β mRNA was analyzed by RT-qPCR (**E** and **G**) the corresponding fold inductions were calculated with respect to mock-transfected, non-treated and NDV-infected cells (n=3). Student test: p-value less than 0.001 (***) and 0.01 (**). All images correspond to one confocal section. Scale bar = 10μM.

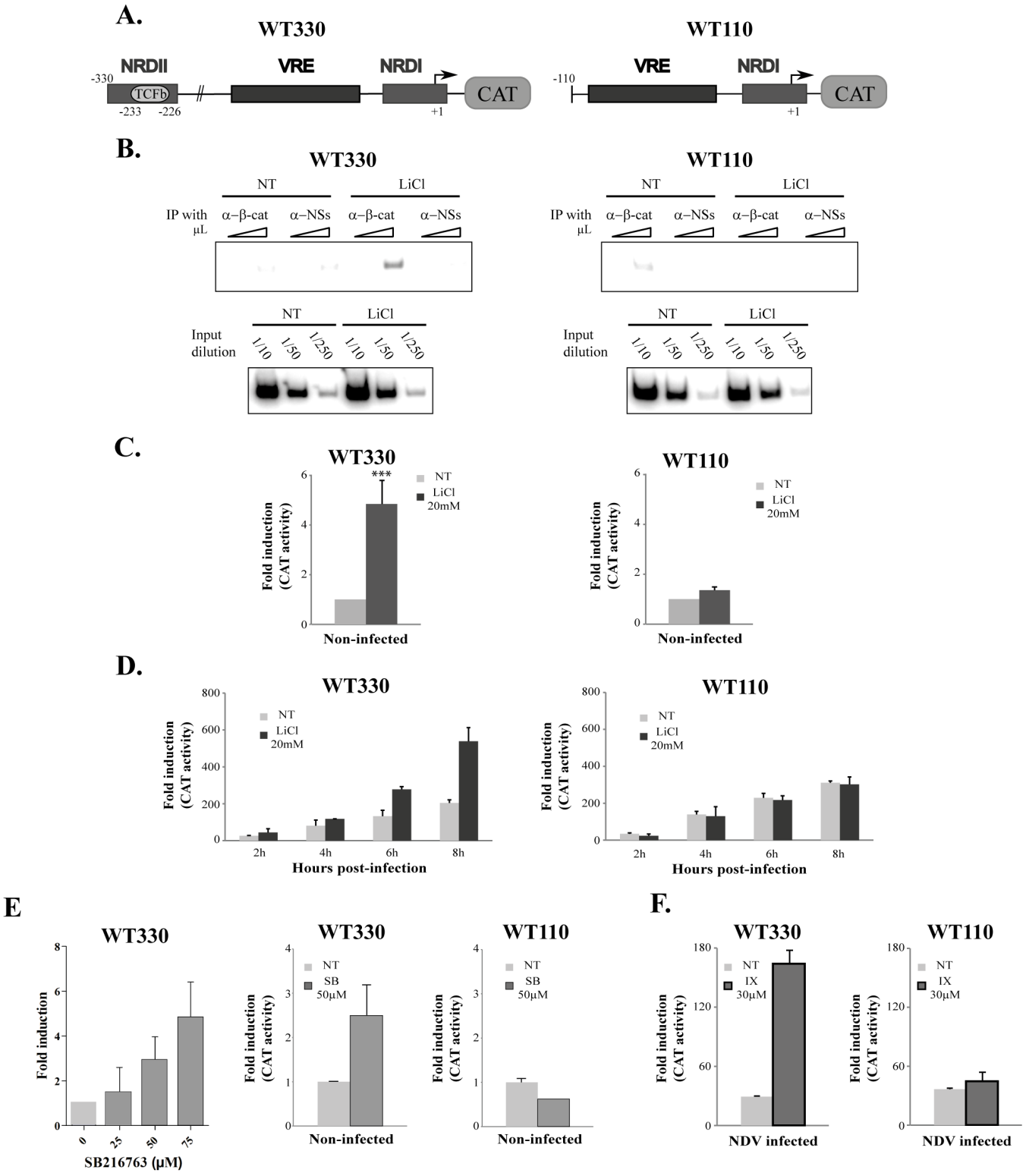

Figure 3. Interaction of β-catenin with the IFN-β promoter region containing a TCF binding site is necessary for LiCl enhancement of IFN-β promoter activity. (**A**) Schematic representation of the WT330 and WT110 murine IFN-β promoters fused to the CAT reporter gene and integrated into the genome of L929 WT330 and L929 WT110 cell lines respectively. (**B** to **D**) β-catenin binding to WT330 and WT110 promoters and corresponding CAT activities were analysed in L929 WT330 and WT110 cells either non-treated (NT) or treated with LiCl 20mM (LiCl). (**B**) Genomic DNA was collected 24h post-LiCl treatment and immunoprecipited with anti β-catenin (α-β-cat) or anti NSs (α-NSs, negative control) antibodies. Increasing amounts of immunuprecipitated DNA (IP), as well as non immunoprecipitated genomic DNA (Input) were amplified by semi-quantitative PCR using specific primers for the WT330 and WT110 integrated promoters. (**C**) Cells were collected post-LiCl treatment and their CAT activities quantified. The corresponding fold inductions were calculated with respect to non-treated cells (n=12 for WT330 and n=6 for WT110 cell lines). (**D**) Post-LiCl treatment, cells were further mock- or NDV-infected, collected at different times post-infection and the corresponding CAT activities were quantified. The corresponding fold inductions were calculated with respect to non-infected non-treated cells (n=4). (**E** and **F**). CAT activities of L929 cells either non-treated (NT) or treated with 50μM of SB 216763 (**E**) or 30μM of IX inhibitor during 24h. (**F**). Cells were further mock or NDV-infected, collected 8h post-infection and the corresponding CAT activities quantified. The corresponding fold inductions were calculated with respect to non-infected non-treated cells.

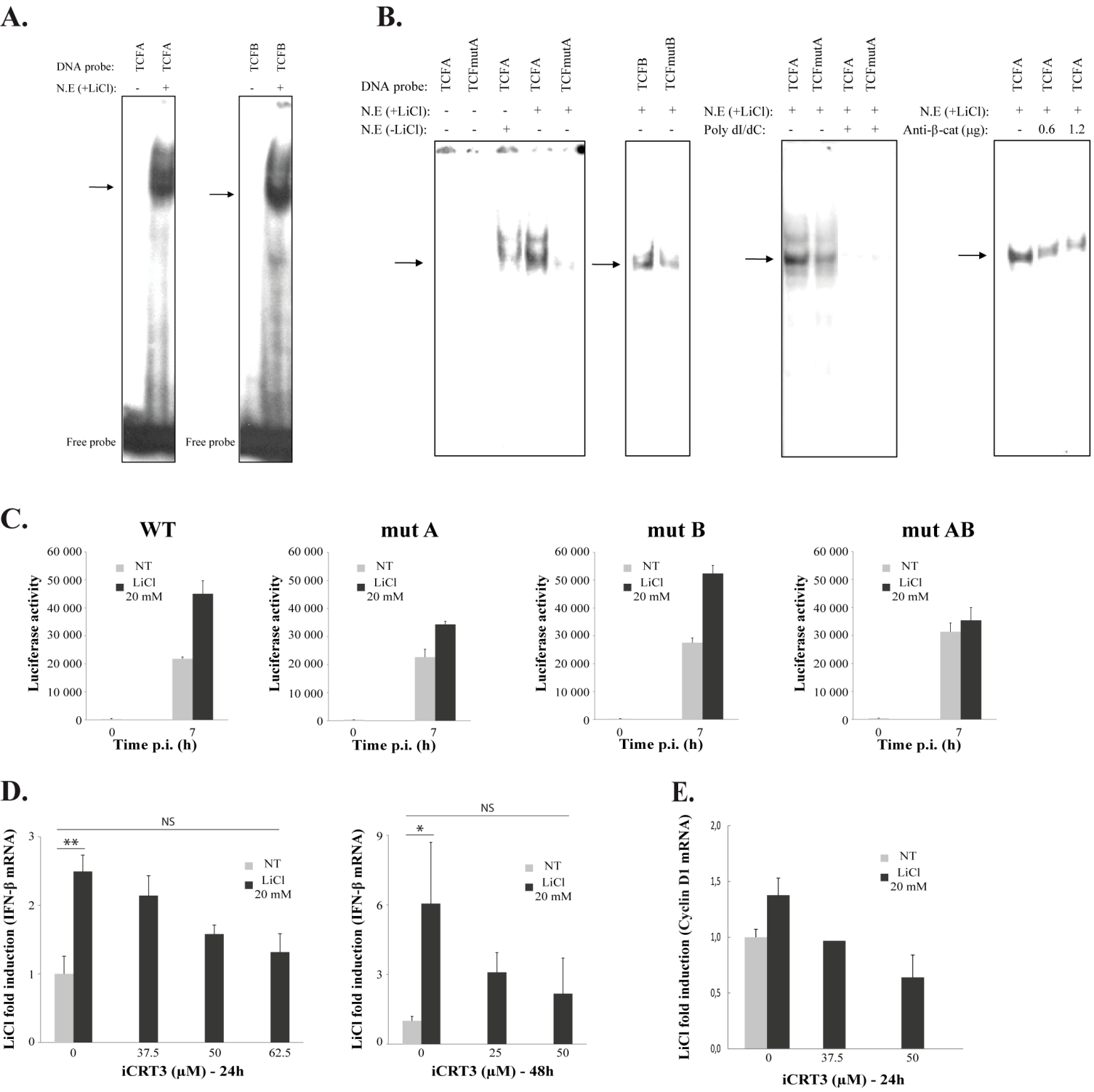

Figure 4. TCF binding sites mediate LiCl-dependent activation of the IFN-β promoter. (**A and B**) Equal amounts of nuclear extracts (N.E) prepared from L929 either non-treated (-LiCl) or treated with 20mM LiCl (+LiCl) during 24h were incubated with the radioactively labeled probes corresponding to wild type TCFa (TCFA) and TCFb (TCFB) or mutated TCFa (TCFmutA) and TCFb (TCFmutB) sites. When indicated, nuclear extracts were incubated with 500ng of poly dI/dC or anti-β-catenin antibodies before adding the probes. (**C**) L929 cells transfected with plasmids containing luciferase reporter gene under the control of the IFN-β promoter either WT or mutated at the TCFa site (mutA), the TCFb site (mutB) or the TCFa and b sites (mutAB) were either non-treated (NT) or pre-treated with LiCl (LiCl) before infection with NDV. Cells were collected 7h p.i. and the luminescence was quantified with n=3. (**D** and **E**) L929 cells were either non-treated (NT) or treated with 20mM LiCl (LiCl) during 24h or 48h in the presence or absence of iCRT3 before being NDV-infected. IFN-β (**D**) or cyclin D1 (**E**) mRNA was analyzed by RT-qPCR and the corresponding fold inductions were calculated with respect to non-treated NDV-infected (**D**) or non infected (**E**) cells; in D (n=3).
Student test: p-value less than 0.01 (**) and 0.05 (*).

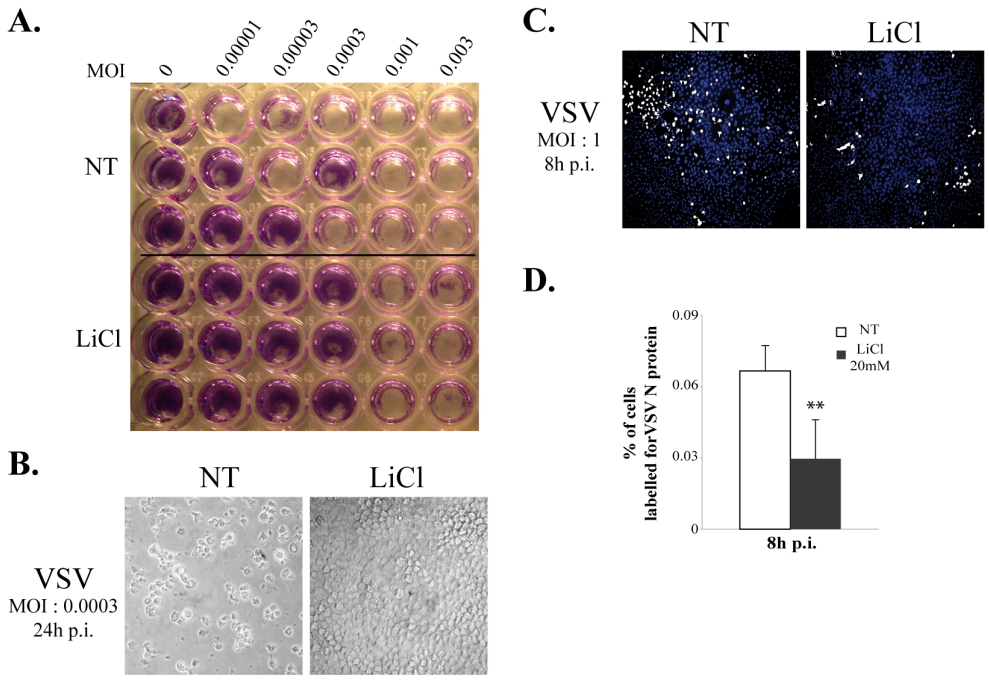

Figure 5. LiCl treatment confers an antiviral state. Monolayers of L929 cells either non-treated (NT) or pre-treated with LiCl 20mM for 24h were infected with VSV. (**A**) Cytopathic effect induced by increasing MOI of VSV was assayed by crystal violet dye staining 24h after infection; (**B**) Photographs of typical culture fields. (**C** and **D**) Cells were fixed 8h after infection (MOI=1), labeled with an antibody directed against the N protein of VSV (displayed in gray) and ToPro3 (blue); merge images of the corresponding culture fields are displayed in (**C**). The % of infected cells, as determined by the presence of N protein encoded by VSV (fluorescence displayed in gray) was determined from a total of 7876 untreated and 9024 LiCl-treated cells counted with n = 4 (**D**).

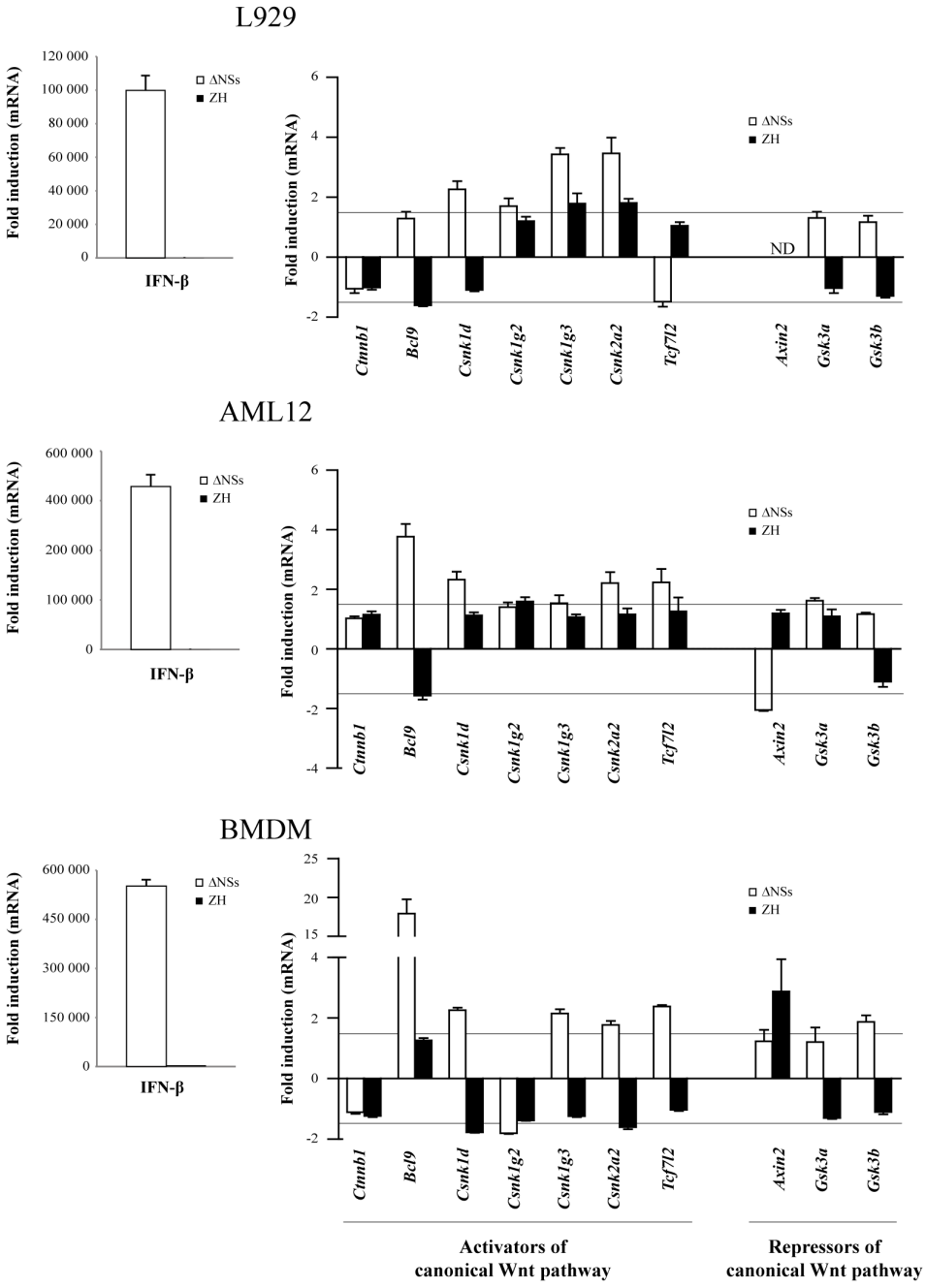

Figure 6. Infection with RVFV affects the Wnt/β-catenin pathway at the transcriptional level.
The expression of genes associated to the Wnt/β-catenin pathway previously identified as interacting with the NSs protein of RVFV (listed in Table II) was measured in three different cell types corresponding to fibroblast (L929), hepatocytes (AML12) and Bone Marrow Derived Macrophages (BMDM) either mock-, RVFZH548- (ZH) or RVFVΔNSs- (ΔNSs) infected. RNAs purified from mock- or virus-infected cells (8h p.i.) were analyzed by RT-qPCR with primers specific for each gene of interest. The change in gene expression was calculated in ZH and ΔNSs-infected cells with respect to mock-infected cells. The horizontal broken lines indicate the cutoff value for upregulation (+1.5 fold) and downregulation (-1.5 fold). The effect of virus infection upon the expression of genes coding for WNT ligands as well as for antagonist of Wnt signaling (Apcdd1, Dkk1 and Kremen2) could not be tested since the corresponding mRNA remained undetectable in the three cell types analyzed here. n≥3 for each cell line.

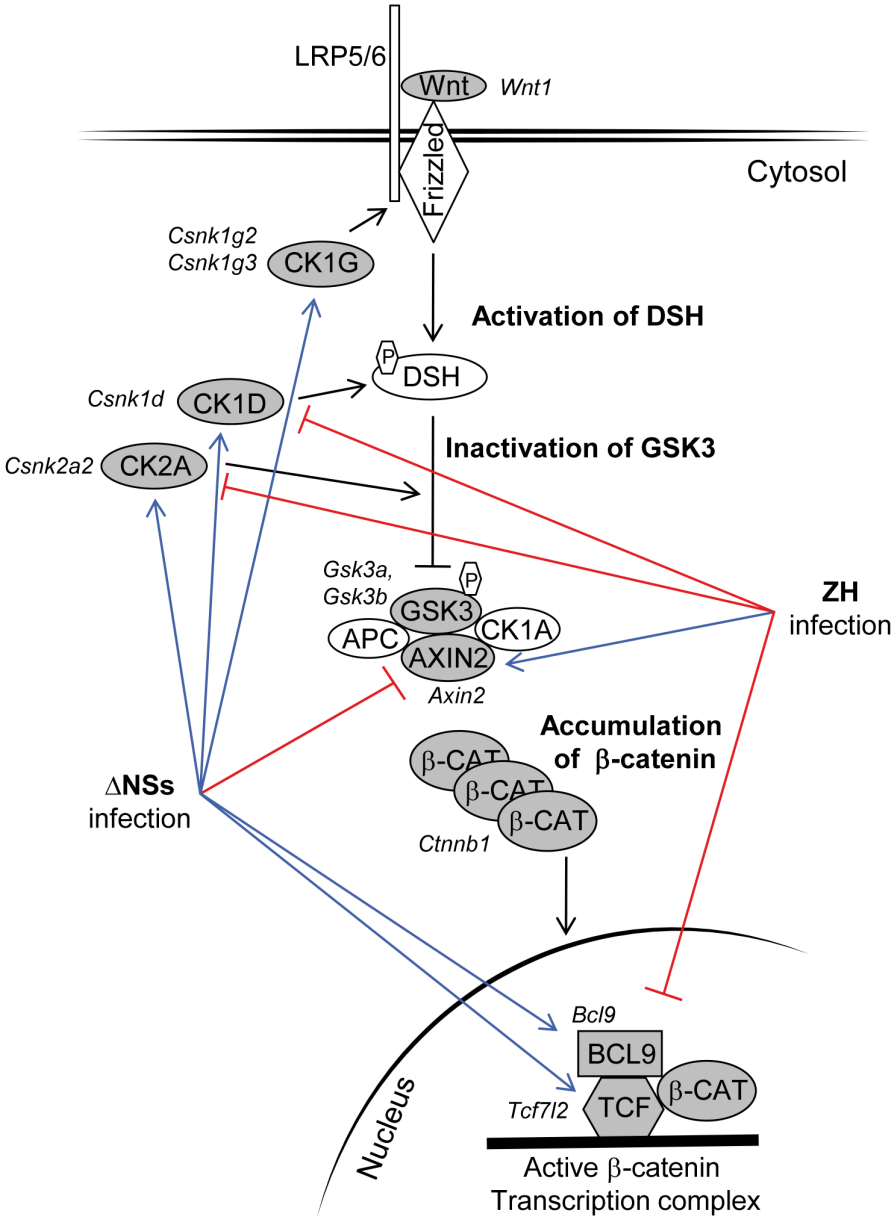

Figure 7. Non-pathogenic and pathogenic strains of RVFV have opposite effects on the Wnt/β-catenin pathway. Genes participating in the Wnt/β-catenin pathway whose promoter regions were identified as significantly interacting with RVFV NSs protein during ChIP-on-chip experiments, listed in Table II, are shown in gray. Genes whose expressions were affected after infection with either the non-pathogenic ΔNSs or the pathogenic ZH strain of RVFV with respect to mock-infected cells are indicated by blue (upregulated) or red (downregulated) arrows.

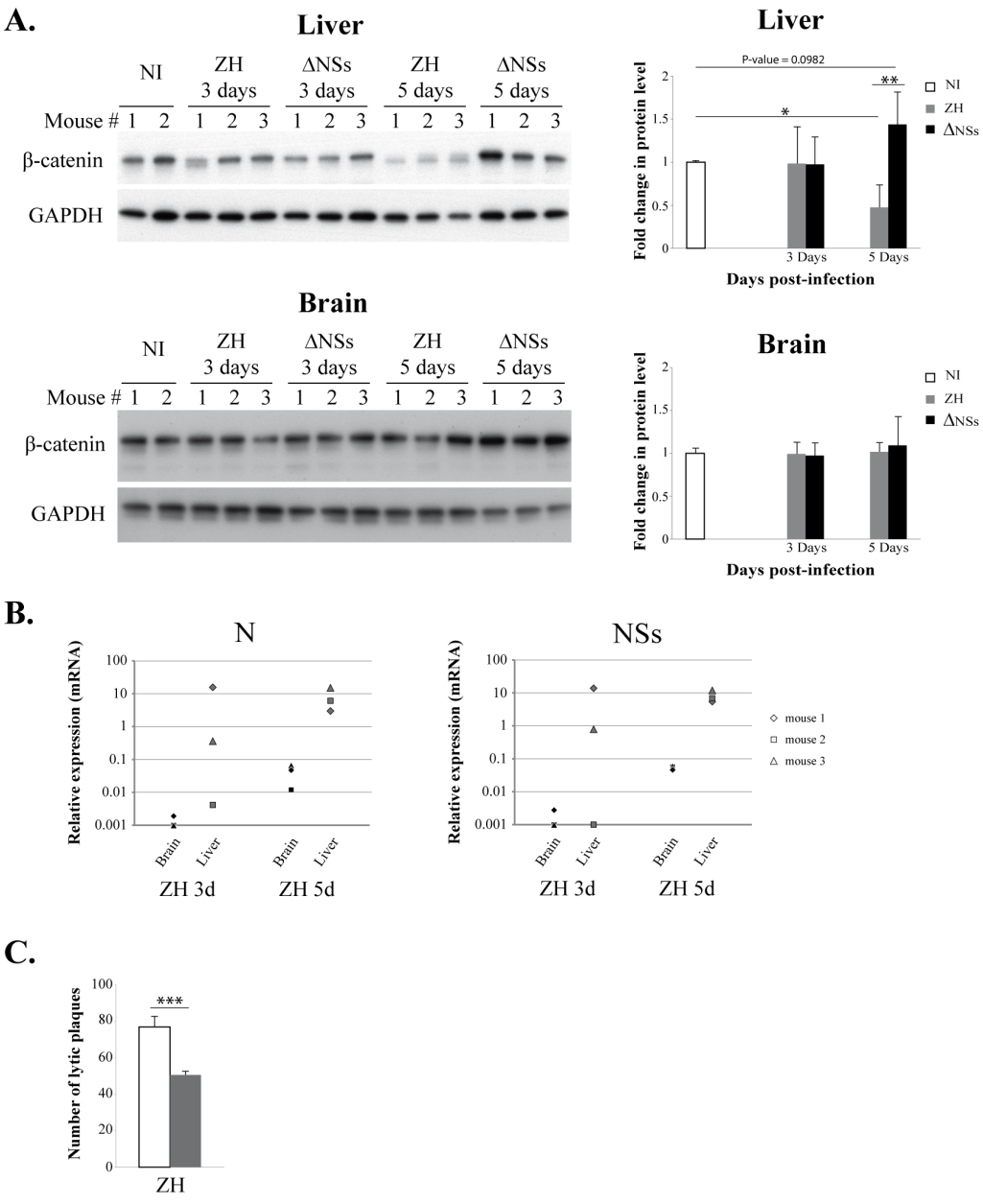

Figure 8. A physiological relevance for β-catenin protein level during RVFV infection. (**A** and **B**) β-catenin protein and viral N and NSs RNA levels were evaluated in liver and brain of mice either non-infected (NI) or at days 3 and 5 p.i. with RVFVZH548 (ZH) or RVFVΔNSs (ΔNSs). (**A**) β-catenin protein level was analysed by Western blot and estimated densitometrically by comparison with the band intensity of GAPDH; fold changes in protein level were calculated by comparison of the relative β-catenin level in infected versus non-infected (NI) samples. Values were averaged from (n) independent samples per time point with n=3 mice (NI), n=6 mice (ZH 3 days and ΔNSs 3 and 5 days) and n=4 mice (ZH 5 days). (**B**) The relative level of viral N and NSs mRNA were estimated by comparison with the expression of three reference genes (Ppib, Hprt1 and Utp6c). (**C**) Number of lytic plaques formed in monolayers of L929 cells either non-treated or pre-treated with LiCl 20 mM during 24h and infected with RVFVZH548. Cells were fixed and stained with crystal violet 3 days p.i. (n=4). Student test: p-value less than 0.001 (***) 0.01 (**) and 0.05 (*).